Geochemistry Geophysics Geosystems G3

Article
Volume 14, Number 10
4 October 2013
doi: 10.1002/ggge.20250
ISSN: 1525-2027

Published by AGU and the Geochemical Society

The composition and distribution of the rejuvenated component across the Hawaiian plume: Hf-Nd-Sr-Pb isotope systematics of Kaula lavas and pyroxenite xenoliths

Michael Bizimis
Department of Earth and Ocean Sciences, University of South Carolina, Columbia, South Carolina 29208, USA (mbizimis@geol.sc.edu)

Vincent J. M. Salters
National High Magnetic Field Laboratory and Department of Earth, Ocean and Atmospheric Sciences, Florida State University, Tallahassee, Florida, USA

Michael O. Garcia
Department of Geology and Geophysics, University of Hawaii, Honolulu, Hawaii, USA

Marc D. Norman
Research School of Earth Sciences, Australian National University, Canberra, ACT, Australia

[1] Rejuvenated volcanism refers to the reemergence of volcanism after a hiatus of 0.5–2 Ma following the voluminous shield building stage of Hawaiian volcanoes. The composition of the rejuvenated source and its distribution relative to the center of the plume provide important constraints on the origin of rejuvenated volcanism. Near-contemporaneous lavas from the Kaula-Niihau-Kauai ridge and the North Arch volcanic field that are aligned approximately orthogonally to the plume track can constrain the lateral geochemical heterogeneity and distribution of the rejuvenated source across the volcanic chain. Nephelinites, phonolites and pyroxenite xenoliths from Kaula Island have radiogenic Hf, Nd and unradiogenic Sr isotope compositions consistent with a time-integrated depleted mantle source. The pyroxenites and nephelinites extend to the lowest $^{208}Pb/^{204}Pb$ reported in Hawaiian rocks. These data, along with new Pb isotope data from pyroxenites from the Salt Lake Crater (Oahu) redefine the composition of the depleted end-member of the Hawaiian rejuvenated source at $^{208}Pb/^{204}Pb=37.35\pm0.05$, $^{206}Pb/^{204}Pb=17.75\pm0.03$, $\varepsilon_{Nd}=9$–10, ε_{Hf} ~16–17 and $^{87}Sr/^{88}Sr$ <0.70305. The revised isotope composition also suggests that this depleted component may contribute to LOA and KEA trend shield stage Hawaiian lavas, consistent with the rejuvenated source being part of the Hawaiian plume and not entrained upper mantle. The isotope systematics of rejuvenated magmas along the Kaula-Niihau-Kauai-North Arch transect are consistent with a larger proportion of the rejuvenated depleted component in the periphery of the plume track rather than along its axis.

Components: 14,286 words, 9 figures, 1 table.

Keywords: pyroxenite; xenolith; rejuvenated volcanism; mantle plume; Kaula; plume structure.

Index Terms: 1038 Mantle processes: Geochemistry; 1033 Intra-plate processes: Geochemistry; 1065 Major and trace element geochemistry: Geochemistry; 1040 Radiogenic isotope geochemistry: Geochemistry; 1025 Composition of the mantle: Geochemistry; 3615 Intra-plate processes: Mineralogy and Petrology; 3621 Mantle processes: Mineralogy and Petrology; 8415 Intra-plate processes: Volcanology.

Received 15 May 2013; **Revised** 13 August 2013; **Accepted** 13 August 2013; **Published** 4 October 2013.

Bizimis, M., V. J. M. Salters, M. O. Garcia, and M. D. Norman (2013), The composition and distribution of the rejuvenated component across the Hawaiian plume: Hf-Nd-Sr-Pb isotope systematics of Kaula lavas and pyroxenite xenoliths, *Geochem. Geophys. Geosyst*, *14*, 4458–4478, doi:10.1002/ggge.20250.

1. Introduction

[2] The Hawaiian-Emperor Chain is the type example of a deep-seated mantle plume [*Morgan*, 1971; *Sleep*, 1990]. Numerous studies have discussed the spatial and temporal distribution of the various compositional components recognized in the Hawaiian lavas, resulting in plume structure models that vary from a concentrically zoned [*DePaolo et al*., 2001] to vertically and laterally asymmetrically heterogeneous plume [*Abouchami et al*., 2005; *Xu et al*., 2007; *Farnetani and Hofmann*, 2010; *Hanano et al*., 2010; *Pietruszka et al*., 2011]. There is, however, considerable debate over the nature and scale of lithological complexity of the Hawaiian plume. For example, several studies suggest that the Hawaiian plume contains recycled eclogite or pyroxenite along with peridotite [*Hauri*, 1996; *Lassiter and Hauri*, 1998; *Blichert-Toft et al*., 1999; *Huang and Frey*, 2005; *Sobolev et al*., 2005], whereas others have argued for the presence of ancient depleted peridotite [*Norman and Garcia*, 1999; *Stracke et al*., 1999; *Kogiso et al*., 2003; *Bizimis et al*., 2005; *Frey et al*., 2005; *Salters et al*., 2006; *Bizimis et al*., 2007]. These models are not mutually exclusive.

[3] The temporal evolution of many Hawaiian volcanoes includes a main phase of voluminous shield-building tholeiitic basalts followed by renewed volcanism after a hiatus of 0.5–2 Ma [*Ozawa et al*., 2005]. The lavas erupted during this rejuvenated stage are alkalic, e.g., alkali basalts to nephelinites [*Clague and Frey*, 1982; *Dixon et al*., 2008; *Garcia et al*., 2010], some with mantle xenoliths [*White*, 1966; *Jackson and Wright*, 1970]. In addition to the subaerial rejuvenated volcanism on the islands there is also widespread and near synchronous submarine alkalic volcanism on the flanks and distal aprons of some islands and along segments of the Hawaiian Arch that is geochemically similar to the rejuvenated volcanism [*Lipman et al*., 1989; *Clague et al*., 1990; *Clague and Dixon*, 2000; *Frey et al*., 2000; *Yang et al*., 2003; *Garcia et al*., 2008]. An important aspect of the rejuvenated volcanism is that it typically has more depleted isotope characteristics (e.g., lower $^{87}Sr/^{86}Sr$, higher $^{143}Nd/^{144}Nd$, higher $^{176}Hf/^{177}Hf$) relative to shield stage basalts and that of primitive mantle [*Stille et al*., 1983; *Frey et al*., 2000; *Frey et al*., 2005; *Fekiacova et al*., 2007; *Garcia et al*., 2010]. The large geographical distribution and the near contemporaneous eruption of rejuvenated type lavas along 300 km of the Hawaiian Chain and on the Hawaiian Arch 200–250 km from the Islands within the last 1 million years [*Garcia et al*., 2010] suggests that the mechanism(s) and source(s) responsible for the rejuvenated volcanism extend over a wide area. The source of rejuvenated volcanism is thought to be the oceanic lithosphere [e.g., *Lassiter et al*., 2000] that has been metasomatized by melts from the plume [*Yang et al*., 2003; *Dixon et al*., 2008] or a source entirely within the mantle plume [*Fekiacova et al*., 2007]. Rejuvenated volcanism, therefore, provides key constraints on the compositional complexity and geodynamics of the Hawaiian plume.

[4] Mantle xenoliths found within the Hawaiian rejuvenated lavas provide additional constraints on the geochemical diversity of the Hawaiian plume and the origin of the rejuvenated volcanism. The garnet pyroxenite xenoliths from Salt Lake Crater (SLC), a vent on Oahu related to the Honolulu Volcanics, are thought to be high pressure ($>$ 20 kb) crystal fractionates from alkali magmas [*Frey*, 1980; *Sen*, 1987; *Keshav and Sen*, 2001; *Bizimis et al*., 2005; *Keshav et al*., 2007; *Sen et al*., 2011]. Thus, they provide access to trapped melts within the lithosphere and potentially allow identification of sources not yet recognized in the surface volcanism. For example, their Hf-Nd isotope systematics suggest the presence of a depleted component within the Hawaiian plume that is distinct from the mantle source of Pacific MORB [*Bizimis et al*., 2005].

[5] Here we present the first combined isotope (Hf, Nd, Sr, Pb), investigation of alkali lavas and pyroxenite xenoliths, including garnet pyroxenites, from

Kaula Island. We also report Pb isotope data on previously described garnet pyroxenite xenoliths from Salt Lake Crater [*Bizimis et al*., 2005; *Sen et al*., 2010; *Sen et al*., 2011], as well as Hf, Nd, Sr, Pb isotopes on two SLC garnet pyroxenites. Kaula Island is at the W-SW end of the Kauai-Niihau-Kaula ridge, which is near orthogonal to the plume track. Thus, data from the rejuvenated Kaula lavas, together with existing data from Niihau, Kauai and North Arch volcanic fields can provide important constraints on the composition of the rejuvenated source across the plume track. Our new data redefine the composition of the depleted rejuvenated component in the plume and show a greater proportion of the depleted component at the periphery than the plume center.

2. Geological Setting and Sample Description

[6] Kaula Island is located ~33 km southwest from the island of Niihau and ~120 km from the center of Kauai. The Kauai-Niihau-Kaula islands form a volcanic ridge that is approximately orthogonal to the Hawaiian ridge (Figure 1). Kaula Island is a 0.5 km^2 remnant of a palagonitic tuff cone with accidental blocks of tholeiite, phonolite, basanite, peridotite, and pyroxenite [*Garcia et al*., 1986]. Nephelinite is the host lava for the blocks. The petrology, major and trace element chemistry of the Kaula volcanics were reported in *Garcia et al*. [1986]. Mineralogy and chemistry of few pyroxenite xenoliths were described by *Garcia and Presti* [1987]. The phonolites were dated by K-Ar methods at 4.0–4.2 Ma [*Garcia et al*., 1986], which is older than the rejuvenated volcanism on the neighboring Niihau and Kauai islands [*Sherrod et al*., 2007; *Garcia et al*., 2010] but overlaps with the shield-to-postshield transition on Kauai. Thus, the phonolites are considered products of postshield stage volcanism [*Garcia et al*., 2010]. A basanite accidental block from Kaula gave an age of 1.8 Ma [*Garcia et al*., 1986] overlapping with the rejuvenated volcanism in the adjacent islands [*Garcia et al*., 2010]. Nephelinitic juvenile bombs have not been dated but their eruption age is assumed to be younger than the 1.8 Ma basanite accidental block. The similar major and trace element composition of the Kaula nephelinites and basanites with the rejuvenated lavas from Oahu and Kauai, the overlap of eruption ages for Kaula

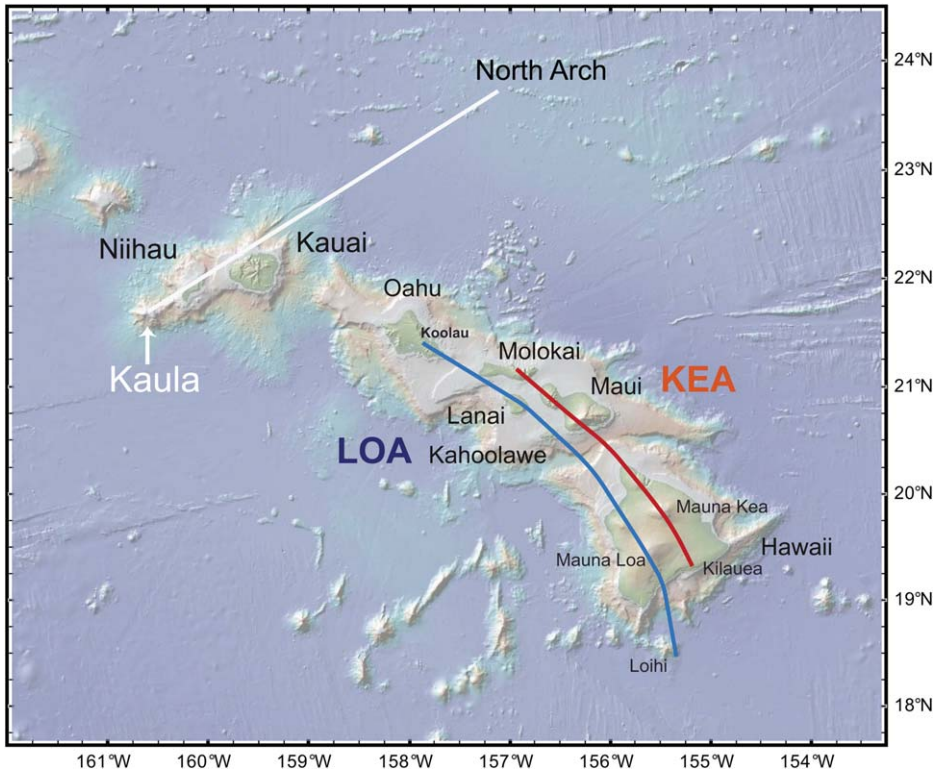

Figure 1. Bathymetric map of the Hawaiian Islands (USGS: http://geopubs.wr.usgs.gov/i-map/i2809/). The loci of the LOA and KEA trend volcanoes are after *Jackson et al*. [1972]. The white line shows the approximate strike of the Kaula-Niihau-Kauai ridge and North Arch volcanic field.

with the Kauai and Niihau rejuvenated volcanism and the presence of xenoliths, suggest that the Kaula lavas are related to the rejuvenated volcanism [*Garcia et al*., 1986]. Here we report Hf, Nd, Sr, Pb isotope data on three nephelinites and three phonolites including sample KA-36 that was dated at 4.22± 0.25 [*Garcia et al*., 1986].

[7] The Kaula pyroxenite xenoliths are clinopyroxenites (samples KA-51, 72, 73, 102, 103, 104) with clinopyroxene and orthopyroxene at >50 and <40 volume percent modal abundance respectively, and garnet-bearing clinopyroxenites (up to 19 volume percent modal garnet, samples KA-107, 106, 107 109). Olivine and spinel are present from trace amounts to a few volume percent; phlogopite occurs in trace amounts in few samples [*Presti*, 1982]. Glass patches occur in some pyroxenites and were explained as a reaction with nephelinite host melt [*Garcia and Presti*, 1987]. The major element chemistry and petrography of the Kaula pyroxenites were originally reported in *Presti* [1982]. We conducted additional mineral major and trace element analyses along with Hf, Nd, Sr, Pb isotope data on clinopyroxenes. The SLC pyroxenites are from the Presnall and Jackson collections housed at the Smithsonian Institution [*Bizimis et al*., 2005; *Keshav et al*., 2007].

3. Analytical Methods

[8] Mineral major element compositions were determined either with a 5 spectrometer JEOL 8500F electron microprobe at the University of Hawaii, or on the 5 spectrometer JEOL Superprobe (JSM 8900R) at the FCAEM, Florida International University, following *Keshav and Sen* [2001] and *Keshav et al*. [2007]. Some analyses are taken from the study of *Presti* [1982] using a five spectrometer SX-50 at the University of Hawaii and are reported here for completeness. All of the data are reported in the supporting information[1].

[9] Trace element analyses in clinopyroxene were performed by laser ablation inductively coupled plasma mass spectrometry (LA-ICPMS) either at RSES-ANU using an excimer 193 nm laser coupled to an Agilent 7500 quadrupole ICPMS, or at NHMFL-FSU with a NEW WAVE 213 nm Nd:YAG laser coupled to an Element 1 High Resolution ICPMS using previously reported procedures [*Norman et al*., 2004; *Bizimis et al*., 2007]. Trace element concentrations are reported in the supporting information.

[10] Chemical separations and isotope ratio determinations were performed at the Geochemistry Division, National High Magnetic Field laboratory, Florida State University (NHMFL/FSU), and at the Center for Elemental Mass Spectrometry (CEMS), Department of Earth and Ocean Sciences, University of South Carolina. Clinopyroxene was separated from the pyroxenites by a combination of crushing, magnetic separation and picking under a binocular microscope. The clinopyroxene separates where leached in 6N HCl at ~100°C for several hours and then rinsed with 18MΩ H_2O. 100 mg of hand crushed millimeter-sized chips from some lava samples were picked under the microscope and leached in warm 2.5 N HCl for 1 h to remove possible contamination during sample processing. The chips were dissolved without further powdering. Some lava samples were already powdered and were not leached. Pb isotope compositions of duplicate chip and powder splits gave within error identical values, suggesting no analytical bias between the two processes. All samples were dissolved in Teflon beakers with HF:HNO3 mixture. Pb was extracted using HNO_3-HBr acids in anion resin [*Manhès et al*., 1984]. The eluent from the Pb columns was processed for Hf isotopes after *Munker et al*. [2001]. Sr and Nd were subsequently separated from the Hf column bulk rock eluent using conventional cation exchange methods, while Nd was further separated from the REE using the Ln-resin (Eichrom, USA).

[11] Sr isotopes were determined on a Finnigan MAT 262 thermal ionization mass spectrometer (TIMS). The Eimer and Amend (E&A) $SrCO_3$ standard was determined at $^{87}Sr/^{86}Sr = 0.708000 \pm 0.000015$ (2 standard deviations: 2 stdv, n=15). Nd-isotopes were determined either on the Finnigan MAT 262 TIMS or a Thermo Neptune multi collector ICPMS (MC-ICPMS) at NHMFL/FSU. The LaJolla Nd standard gave $^{143}Nd/^{144}Nd$=0.511846 ± 0.000011 (2 stdv, n=10) by TIMS. On the MC-ICPMS sample introduction was by a 50 ul PFA self-aspirating nebulizer coupled to an ESI Apex® introduction system. The LaJolla standard was run every two to three samples. All Nd measurements were fractionation corrected to $^{146}Nd/^{144}Nd = 0.7219$ and normalized to $^{143}Nd/^{144}Nd = 0.511850$ for the LaJolla standard. Blanks were Nd ~10pg and Sr < 100pg.

[12] Pb isotope ratios where determined on the Neptune MC-ICPMS or on the FinniganMAT 262 TIMS. On the MC-ICPMS, Pb isotopes were determined with the Tl addition method [*White et al*., 2000] using $^{203}Tl/^{205}Tl = 0.418911$

to correct for mass fractionation. The NBS 981 Pb standard was determined at $^{206}Pb/^{204}Pb = 16.928 \pm 0.003$, $^{207}Pb/^{204}Pb = 15.482 \pm 0.003$, $^{208}Pb/^{204}Pb = 36.669 \pm 0.006$ (2 stdv, $n = 16$), and the sample Pb isotope ratios are reported relative to the NBS 981 values of *Todt et al*. [1996]. For the TIMS measurements, all reported Pb isotope ratios were determined on a single analytical session and the data are corrected for fractionation by 0.081 %/amu, based on replicate measurements of the NBS 981 standard and the values reported in *Todt et al*. [1996]. External reproducibility of the standard was 0.04%/amu (n=6). Duplicate clinopyroxene samples run with both methods agree within internal error. Blanks for Pb were ~50 pg.

[13] The Hf isotope ratios were determined on a Neptune MC-ICPMS at NHMFL/FSU and at CEMS/USC. At FSU the JMC 475 reference solution was determined at $^{176}Hf/^{177}Hf = 0.282149 \pm 9$ (2 stdev, n=30; average of 45–90 ng runs). At USC a spilt from the same solution was determined at $^{176}Hf/^{177}Hf = 0.282142 \pm 5$ (2 stdev, n=10; average of 20 ng runs). All measurements were corrected for fractionation using $^{179}Hf/^{177}Hf = 0.7325$ and are reported relative to the accepted JMC-475 value of $^{176}Hf/^{177}Hf = 0.282160$. Lu and Yb interferences were corrected online using the instrument software. Duplicates run in both labs agree within error. Blanks for Hf were <40pg. The Sr, Nd, Hf, Pb isotope data are reported in Table 1.

4. Results

4.1. Major Element Compositions

4.1.1. Clinopyroxene and Garnet

[14] The clinopyroxenes from Kaula pyroxenites are classified as aluminian augites after *Morimoto* [1988], with relatively Fe-rich (Mg#= 0.73–0.83, where Mg# = Mg/[Mg+Fe] cations) compositions compared to clinopyroxenes from Hawaiian spinel peridotites with Mg#> 0.88 (Figure 2a). The compositions of clinopyroxenes in the Kaula pyroxenites overlap with those in the SLC pyroxenites (e.g., Na_2O versus Mg#, Figure 2a), although the Kaula clinopyroxenes extend to somewhat higher Al contents at a given Mg# (Figure 2b).

[15] The Kaula and SLC pyroxenite garnet compositions entirely overlap (not shown). Some of the Kaula garnets have spinel cores, as also observed in the SLC pyroxenites [*Keshav et al*., 2007]. On a $Mg\#_{cpx}$ versus $Mg\#_{garnet}$ plot, the Kaula samples have slightly higher $Mg\#_{garnet}$ at a given $Mg\#_{cpx}$ than the SLC pyroxenites and the two trends are subparallel (Figure 3a). Experimental data on pyroxenitic and eclogitic compositions [*Hirschmann et al*., 2003; *Kogiso et al*., 2003; *Keshav et al*., 2004; *Pertermann et al*., 2004] show coexisting clinopyroxene-garnet pairs with variable $Mg\#_{cpx}/Mg\#_{gt}$ ratios similar to the SLC and Kaula ranges (Figure 3a). There is no straightforward relationship between $K_D^{Fe\text{-}Mg}$ and P,T or compositional parameters. As the Kaula clinopyroxene-garnet pairs follow the same trend as the SLC, we interpret the Kaula pyroxenite clinopyroxene and garnet compositions to reflect equilibrium conditions.

4.1.2. Orthopyroxene

[16] Orthopyroxene compositions in the Kaula pyroxenites overlap with those of the SLC pyroxenites on a $Mg\#_{cpx}$ versus $Mg\#_{opx}$ plot (not shown), but they extend to higher Al_2O_3 contents at a given Mg# (Figure 3b). In SLC pyroxenites, high-Al orthopyroxenes occur in the contact rims between garnet and spinel [*Keshav et al*., 2007]. This is also observed in the Kaula pyroxenites where the contact rim between spinel and garnet in samples KA-106 and KA-107 contains Al-rich orthopyroxene (Figure 3b, data in the supporting information). These interstitial orthopyroxenes have variable Al contents even within a few 10s of microns. *Garcia and Presti* [1987] suggested that the secondary orthopyroxene in sample KA-107 formed during the reaction of an infiltrating nephelinitic melt with a preexisting garnet + clinopyroxene + spinel mineralogy.

4.2. Trace Element Results

[17] The chondrite-normalized rare earth element (REE) patterns of the Kaula pyroxenite clinopyroxenes show light REE enrichment with convex upward REE patterns, whereas patterns for samples KA-102 and KA-104 are more sinuous (Figure 4a). Compared to the SLC pyroxenites, the Kaula clinopyroxenes generally have higher heavy REE (HREE) concentrations and less fractionated REE patterns. We do not observe any correlation between the degree of HREE depletion in clinopyroxene and the presence of garnet. For example, the two samples with the lowest HREE contents in clinopyroxene (1–2 × chondrite, Figure 4a) do not contain garnet. This was also observed in some SLC pyroxenites [*Bizimis et al*., 2005]. This implies that although these clinopyroxenes were in equilibrium with garnet, garnet is heterogeneously distributed in the rock and not present in the studied centimeter-sized xenoliths. Primitive mantle normalized trace element patterns of the Kaula

Table 1. Isotope Compositions of Volcanic Rocks From Kaula and Clinopyroxene Separates From the Kaula and SLC Pyroxenites

	Notes	$^{87}Sr/^{86}Sr$	2σ	$^{143}Nd/^{144}Nd$	2σ	ε_{Nd}	$^{176}Hf/^{177}Hf$	2σ	ε_{Hf}	$^{206}Pb/^{204}Pb$	2σ	$^{207}Pb/^{204}Pb$	2σ	$^{208}Pb/^{204}Pb$	2σ
Kaula Pyroxenites															
KA-51	cpx	0.703194	7	0.513070	4	8.43	0.283237	11	16.44	17.823	2	15.394	2	37.425	4
KA-52	cpx	0.703266	7	0.513036	6	7.76	0.283163	13	13.37	18.030	1	15.420	1	37.655	4
KA-73	cpx[a]	0.703256	6	0.513049	3	8.02	0.283201	2	14.71	17.957	1	15.427	1	37.602	3
KA-102	cpx[b]	0.703229	8	0.513046	12	7.96	0.283192	10	14.39	18.059	4	15.447	4	37.705	12
KA-102 (dup)	cpx[a]						0.283200	7	14.68						
KA-103	cpx[a]	0.703259	7	0.513047	15	7.98	0.283172	7	13.69	18.021	3	15.442	2	37.612	3
KA-103 (dup)	cpx[b]	0.703254	8				0.283157	11	13.15	18.063	53	15.481	46	37.722	115
KA-104	cpx[b]	0.703243	8	0.513046	11	7.96	0.283175	18	13.79	18.064	15	15.480	14	37.774	36
KA-106	cpx	0.703202	7	0.513069	5	8.41	0.283227	6	15.63	17.823	1	15.418	1	37.449	4
KA-106 (dup)	cpx[b]									17.817	28	15.414	24	37.436	60
KA-107	cpx	0.703228	6	0.513043	3	7.90	0.283190	9	14.32	18.072	1	15.438	1	37.689	3
KA-109	cpx	0.703122	8	0.513088	5	8.78	0.283228	4	15.67	17.801	1	15.422	1	37.419	5
KA-109 (dup)	cpx[a]						0.283228	6	15.67						
SLC Pyroxenites															
77SL-620	cpx[d]									18.095	2	15.442	2	37.726	5
77SL-555	cpx[d]									17.948	1	15.423	1	37.571	3
77SL-714	cpx[d]									18.082	2	15.419	1	37.670	3
77SL-716	cpx[d]									18.055	1	15.431	1	37.582	3
77SL-552	cpx[d]									18.115	2	15.396	2	37.679	6
77SL-776	cpx[d]									18.192	1	15.440	1	37.809	3
NHMN114954-20A	cpx[a]	0.703307	8	0.513032	8	8.88	0.283188	7	14.25	18.148	28	15.452	24	37.762	60
NMNH114954-28A	cpx[a]	0.703165	8	0.513064	6	7.88	0.283266	7	17.01	18.088	2	15.419	1	37.682	3
Kaula Volcanic Rocks															
KA-19	Neph[e]	0.703504	7	0.513024	4	7.53	0.283156	4	13.57	18.0197	6	15.4358	7	37.6713	20
KA-28	Neph[e]	0.703305	13	0.513032	2	7.69	0.283180	3	14.43	17.9556	6	15.4182	7	37.5820	19
KA-34	Neph[e]	0.703502	7	0.513028	2	7.61	0.283186	4	14.64	18.0030	4	15.4339	5	37.6473	14
KA-36	Phon[f]	0.703325	7	0.513039	6	7.82	0.283168	4	14.00	18.0859	6	15.4333	7	37.7296	19
KA-36 (dup)	Phon[c]									18.0988	3	15.4433	4	37.7570	13
KA-37	Phon[f]	0.704018	7	0.513012	7	7.30	0.283185	2	14.61	18.0964	5	15.4395	5	37.7542	16
KA-37 (dup)	Phon[c]									18.0963	4	15.4422	5	37.7597	14
KA-41	Phon[f]	0.703290	7	0.513028	13	7.61	0.283162	3	13.79	18.0877	6	15.4382	7	37.7380	22
USGS Reference Materials															
BIR-1[a]							0.283264	4	16.94	18.8467	5	15.6506	5	38.4724	16
BHVO-1		0.703449	8	0.512972	5	6.5	0.283103	3	11.25	18.6935	4	15.5628	4	38.3372	14
BCR-1		0.705020	8	0.512629	4	−0.2	0.282872	9	3.15						

[a]Hf isotopes at USC, all else at FSU.
[b]Pb isotope by TIMS, all others by MC-ICPMS.
[c]Neph = nephelinite, Phon = Phonolite, (dup) = duplicate. Duplicate dissolution and chemical separation.
[d]Hf, Nd, Sr isotope compositions of the SLC pyroxenites are reported in *Bizimis et al.* [2005]. $2\sigma = 2 * \text{stdev}/\sqrt{n}$ internal precision of the analyses, listed for last significant digits. ε_{Nd} and ε_{Hf} are calculated using CHUR $^{143}Nd/^{144}Nd = 0.512638$, and $^{176}Hf/^{177}Hf = 0.282785$, respectively.
[e]Rock chip.
[f]Powder.

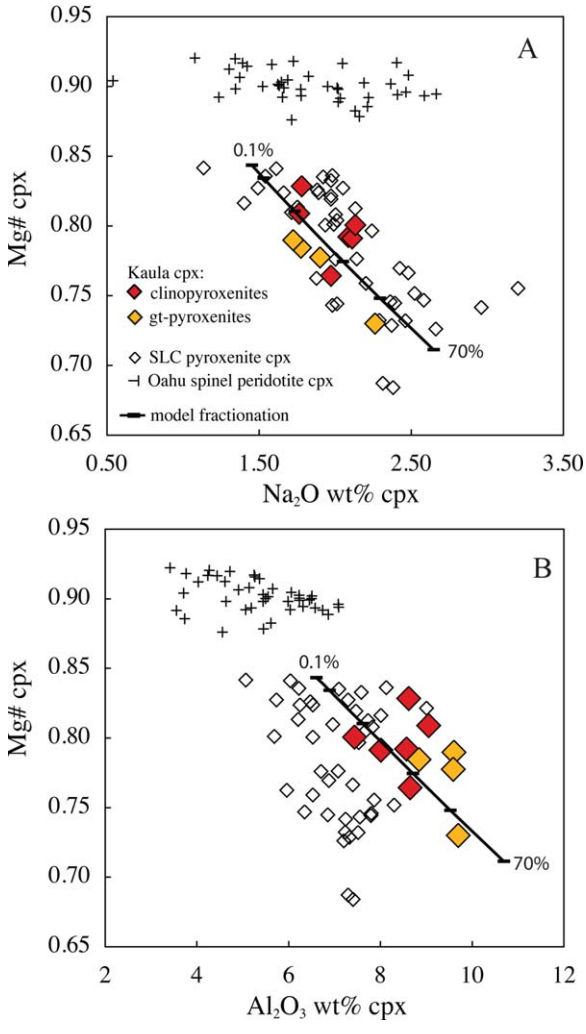

Figure 2. (a) Mg# versus Na_2O wt% and (b) Mg# versus Al_2O_3 wt% in clinopyroxenes from Kaula pyroxenites (red diamonds, orange diamonds are garnet-bearing) compared to clinopyroxenes from SLC pyroxenites (open diamonds) [*Beeson and Jackson*, 1970; *Sen*, 1987; *Sen*, 1988; *Frezzotti et al*., 1992; *Bizimis et al*., 2004; *Keshav and Sen*, 2004; *Bizimis et al*., 2005; *Bizimis et al*., 2007; *Keshav et al*., 2007] and from Oahu spinel peridotite xenoliths (crosses) [*Bizimis et al*., 2004; *Bizimis et al*., 2007]. Line with tick marks (Figures 2a and 2b) shows clinopyroxene model compositions in equilibrium with a fractionating melt. Melt starting composition is Mg#=0.64, $Na_2O = 2.9$ wt%, Al_2O_3=11 wt%, within the range of the Honolulu Volcanics and Kaula nephelinites. Tick marks are at 0.1%, 10%, 30%, 50%, and 70% fractionation, with the 0.1% and 70% labeled. The model assumes fractional crystallization of clinopyroxene only using $D^{Na}_{cpx} = 0.5$, $D^{Al}_{cpx} = 0.6$ and $K_D{}^{Fe/Mg}_{cpx} = 0.35$, approximated from the experimental data of *Walter* [1998] and *Keshav et al*. [2004]. The model reproduces the natural data well. The modeled Al_2O_3 concentrations are sensitive to the choice of the initial Al concentration in the melt and the bulk partition coefficient, which may vary substantially depending on whether garnet is crystallizing together with cpx.

clinopyroxenes show positive Sr and negative Pb anomalies but lower Zr-Hf contents than their SLC counterparts, consistent with their lower LREE and MREE concentrations relative to SLC (Figure 4b).

4.3. Isotope Compositions

4.3.1. Pb Isotope Systematics

[18] The Kaula clinopyroxenes have relatively unradiogenic Pb isotope ratios (Table 1) and extend to lower $^{208}Pb/^{204}Pb$ ratios that previously reported in Hawaiian shield or rejuvenated lavas (Figure 5a). The three most unradiogenic pyroxenites (KA-51, KA-106, KA-109) include both garnet-bearing and garnet-free samples. Thus, there is no apparent correlation between mineralogy and isotope composition. Pb isotope ratios for Kaula nephelinites overlap those of pyroxenites and extend to less radiogenic compositions than other Hawaiian rejuvenated lavas. The Kaula phonolites have slightly more radiogenic Pb isotope ratios than the nephelinites and overlap other rejuvenated lava compositions from Oahu (Honolulu Volcanics), Niihau (Kiekie Volcanics), and the unradiogenic end of the field defined by rejuvenated stage (Koloa Volcanics) and post-shield lavas from Kauai (Figure 5a). The SLC pyroxenite clinopyroxenes partially overlap and extend to less radiogenic Pb isotope ratios than their host Honolulu Volcanics lavas.

[19] In $^{206}Pb/^{204}Pb$ versus $^{208}Pb/^{204}Pb$ space the Kaula and SLC pyroxenites define two slightly offset arrays with slopes that are identical within error (1.1 ± 0.1 and 1.0 ± 0.2, respectively) (Figure 5b). The Koloa Volcanics plot at the radiogenic extension of the Kaula pyroxenite Pb isotope array with a slope of 1.21 ± 0.04 that is within error of the pyroxenites (Figure 5b). Together, the Kaula pyroxenites and lavas and the Koloa Volcanics define an array that is oblique to and crosses the LOA-KEA divide into the LOA field (Figures 5a and 5b). In contrast, the Honolulu Volcanics have a distinctly shallower slope (0.76 ± 0.07) and plot on the KEA side of the divide. The Kalaupapa Volcanics of East Molokai define a slope (0.87 ± 0.20) intermediate to that of the Honolulu Volcanics and the Koloa or Kaula pyroxenites, although with a larger uncertainty due to the limited Pb isotope variability. The North Arch lavas entirely overlap the Kalaupapa lavas Pb isotope values but with only 4 samples and a small range in Pb isotopes it is difficult to obtain meaningful regression lines. Overall, our new Kaula and SLC Pb isotope data, together with

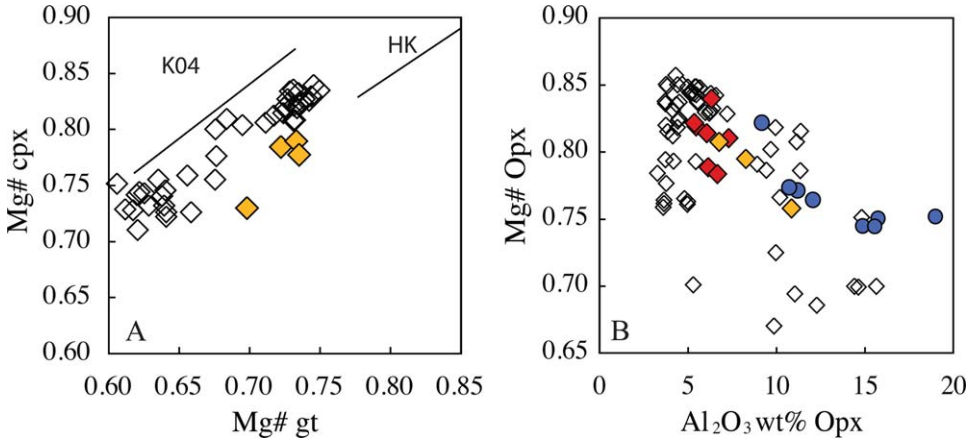

Figure 3. (a) Mg# in clinopyroxenes and coexisting garnets in the Kaula and the SLC pyroxenites. Lines are regression lines through clinopyroxene and garnet compositions from experimental data: K04, [*Keshav et al*., 2004]; H, K03, [*Hirschmann et al*., 2003; *Kogiso et al*., 2003]. Pyroxenite data sources and symbols as in Figure 2. (b) Orthopyroxene Mg# versus Al_2O_3 in the Kaula and SLC pyroxenites. Blue circles are interstitial orthopyroxenes in the Kaula pyroxenites (supporting information); other symbols and data sources as in Figure 2. The interstitial orthopyroxenes have higher Al contents than the cores of large orthopyroxenes, but also overlap some SLC pyroxenite data.

other published rejuvenated lava data forms a well-defined array in $^{206}Pb/^{204}Pb$ versus $^{208}Pb/^{204}Pb$ isotope space that is distinct from the LOA and KEA shield stage trends, with lower $^{208}Pb/^{204}Pb$ at a given $^{206}Pb/^{204}Pb$ than the LOA-shield stage lavas, and distinctly less radiogenic Pb isotopes than KEA-shield stage lavas.

4.3.2. Sr-Nd Isotope Systematics

[20] The Kaula lavas and pyroxenites have relatively radiogenic Nd and unradiogenic Sr isotopes compared to the LOA and KEA trend shield volcanoes and broadly overlap the compositions of rejuvenated stage lavas and pyroxenites xenoliths in $^{87}Sr/^{86}Sr$-ε_{Nd} isotope space (Figure 5c). The nephelinites and phonolites form a subhorizontal trend with variable Sr isotopes at near constant Nd, as also observed in the Honolulu Volcanics. Phonolite KA-37 has higher $^{87}Sr/^{86}Sr$ plotting above the Hawaiian shield and rejuvenated lava fields, but overlaps the other two phonolites in all other isotope compositions. In contrast, the Kaula pyroxenites have higher ε_{Nd} and lower $^{87}Sr/^{86}Sr$ than the lavas and form a well-defined negative trend toward the most radiogenic Nd isotopes reported for Hawaiian rejuvenated volcanism (e.g., North Arch lavas) and overlap with the SLC pyroxenite trend. The combined Kaula-SLC pyroxenite trend appears subparallel to the negative trend defined by the Koloa Volcanics, but shifted to slightly higher $^{87}Sr/^{86}Sr$.

4.3.3. Hf-Nd Isotope Systematics

[21] The Kaula lavas and pyroxenites have relatively radiogenic Hf and Nd compositions and overlap the SLC pyroxenites, Honolulu Volcanics and Koloa Volcanics data. In ε_{Hf} versus ε_{Nd} space the Kaula and SLC pyroxenites form a field that originates at the radiogenic end of the Hawaiian shield stage lava compositions (Mauna Kea lavas) and extends toward relatively radiogenic Hf compositions at a given Nd, away from the Pacific MORB field (Figure 5d). In detail the Kaula pyroxenites have a shallower slope (~2.2) than the SLC pyroxenites (slope ~3.6), but considerably steeper than the terrestrial array (~1.5) and the Pacific MORB (~1.4) (Figure 5d). The Kaula lavas have less variable Hf isotopes than the Kaula pyroxenites with no obvious distinction between nephelinites and phonolites.

5. Discussion

5.1. Pressures and Temperatures of Equilibration of the Kaula Pyroxenite Xenoliths

[22] Equilibration temperatures for the garnet-bearing samples were calculated using the pyroxene-garnet Fe-Mg exchange thermometers [*Ellis and Green*, 1979; *Ganguly et al*., 1996; *Nimis and Grutter*, 2010], and the Ca-in-orthopyroxene and orthopyroxene-clinopyroxene Ca-Mg exchange thermometers [*Brey and Köhler*, 1990; *Nimis and Grutter*, 2010] for all samples. Pressures are calculated with the Al-in orthopyroxene thermobarometer of *Brey and Köhler* [1990] and *Nickel and*

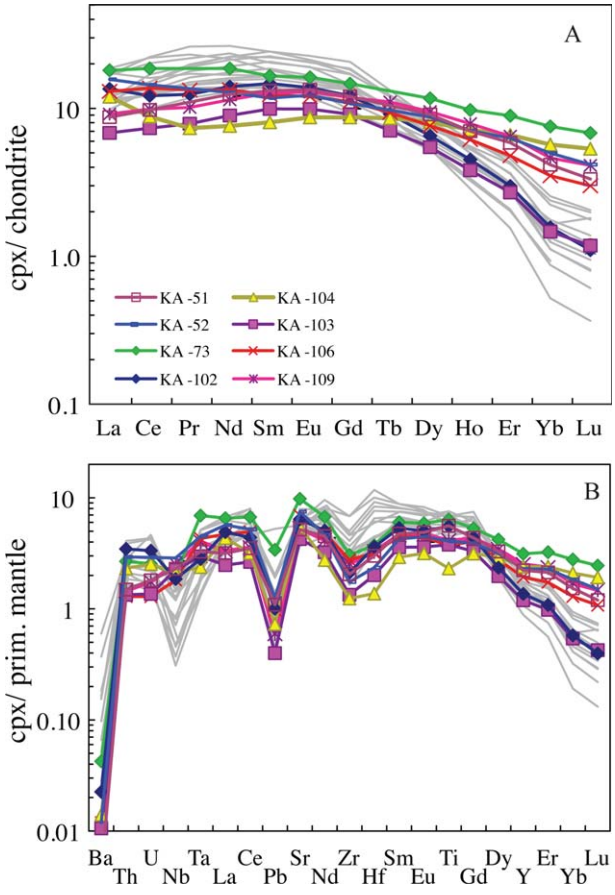

Figure 4. (a) Chondrite normalized REE patterns for the Kaula pyroxenite clinopyroxenes, compared to the SLC pyroxenite data (grey lines with no symbols) [*Bizimis et al.*, 2005]. Normalization values from *Anders and Grevesse* [1989]. (b) Primitive mantle normalized trace element concentrations in the Kaula versus SLC clinopyroxenes. Symbols as in Figure 4a. Normalization values from *McDonough and Sun* [1995].

Green [1985] for the garnet-bearing samples, by solving for pressure and temperature iteratively. For samples without garnet we assume 20 kb pressure. We used the compositions of larger grains and not the interstitial phases. The calculated pressures and temperatures are reported in the supporting information and plotted in Figure 6.

[23] The Ca-in-orthopyroxene and two-pyroxene thermometers give similar temperatures for all samples, around 1100°C. At these temperatures, the calculated pressures for the garnet-bearing samples are relatively low (<13 kb). The orthopyroxene-garnet Fe-Mg thermometer of *Nimis and Grutter* [2010] yields temperatures (~1130 to 1270°C) that are somewhat higher than the pyroxene thermometers and pressures of 11–15 kb. The clinopyroxene-garnet thermometers [*Ellis and Green*, 1979; *Ganguly et al.*, 1996] give temperatures of ~1400 to 1500°C, which are 130–400°C higher than the temperatures derived by the pyroxene thermometers, and result in calculated pressures of 23–25 kb. Such pressures and temperatures would place the Kaula garnet pyroxenites above the peridotite dry solidus [*Hirschmann*, 2000] (Figure 6), so we consider these temperatures unreasonably high. The largest temperature discrepancies between the two pyroxene and clinopyroxene-garnet thermometers are in samples KA-107 and KA-105, which also have opx with the highest Al contents.

[24] An explanation for the temperature (and resulting pressure) differences between the clinopyroxene-garnet and the pyroxene thermometers could be the presence of Fe^{+3} in cpx and garnet. Mossbauer Fe^{3+}/Fe^{2+} data on the SLC pyroxenites [*Tibbetts et al.*, 2010] indicates significant Fe^{3+} contents in cpx (Fe^{+3}/Fe_{total} ~0.3) and garnet (Fe^{+3}/Fe_{total} ~0.05), within the range of clinopyroxenes from cratonic peridotites [*Woodland*, 2009]. Assuming similar Fe^{+3}/Fe_{total} contents in the Kaula clinopyroxenes and garnets, this would result in clinopyroxene-garnet temperatures that are 150–200°C lower than assuming $Fe_{total}= Fe^{+2}$, thus decreasing the discrepancy between the pyroxene and clinopyroxene-garnet thermometers. As the pressure effect on both pyroxene thermometers is relatively small (30°C/10 kb), we take the orthopyroxene-clinopyroxene Ca-Mg exchange thermometer temperatures to broadly reflect those of last equilibration (Figure 6). However, the calculated pressures (8–15 kb) for the garnet pyroxenites are inconsistent with the presence of garnet, which suggests pressures higher that about 18–20 kb in Cr-poor basaltic systems similar to the composition of these pyroxenites [*Sen*, 1988; *Liu and Presnall*, 2000; *Keshav et al.*, 2007].

[25] Additional evidence for the pressure of igneous crystallization may come from phase petrography. Based on experimental data in the CMAS system and the coexistence of olivine +clinopyroxene + garnet it was suggested that the SLC garnet pyroxenites crystallized at >30 kb [*Keshav et al.*, 2007]. Below 30 kb, the olivine +clinopyroxene + garnet assemblage does not exist on the liquidus of the CMAS system [*Milholland and Presnall*, 1998] and the liquidus phases are clinopyroxene, garnet and spinel. Since the Kaula garnet pyroxenites only have traces of olivine they likely crystallized at <30 kb (<90 km), with spinel as the early crystallizing phase as observed experimentally in similar composition systems [*Keshav et al.*, 2004]. The low calculated pressures (<15 kb) and relatively

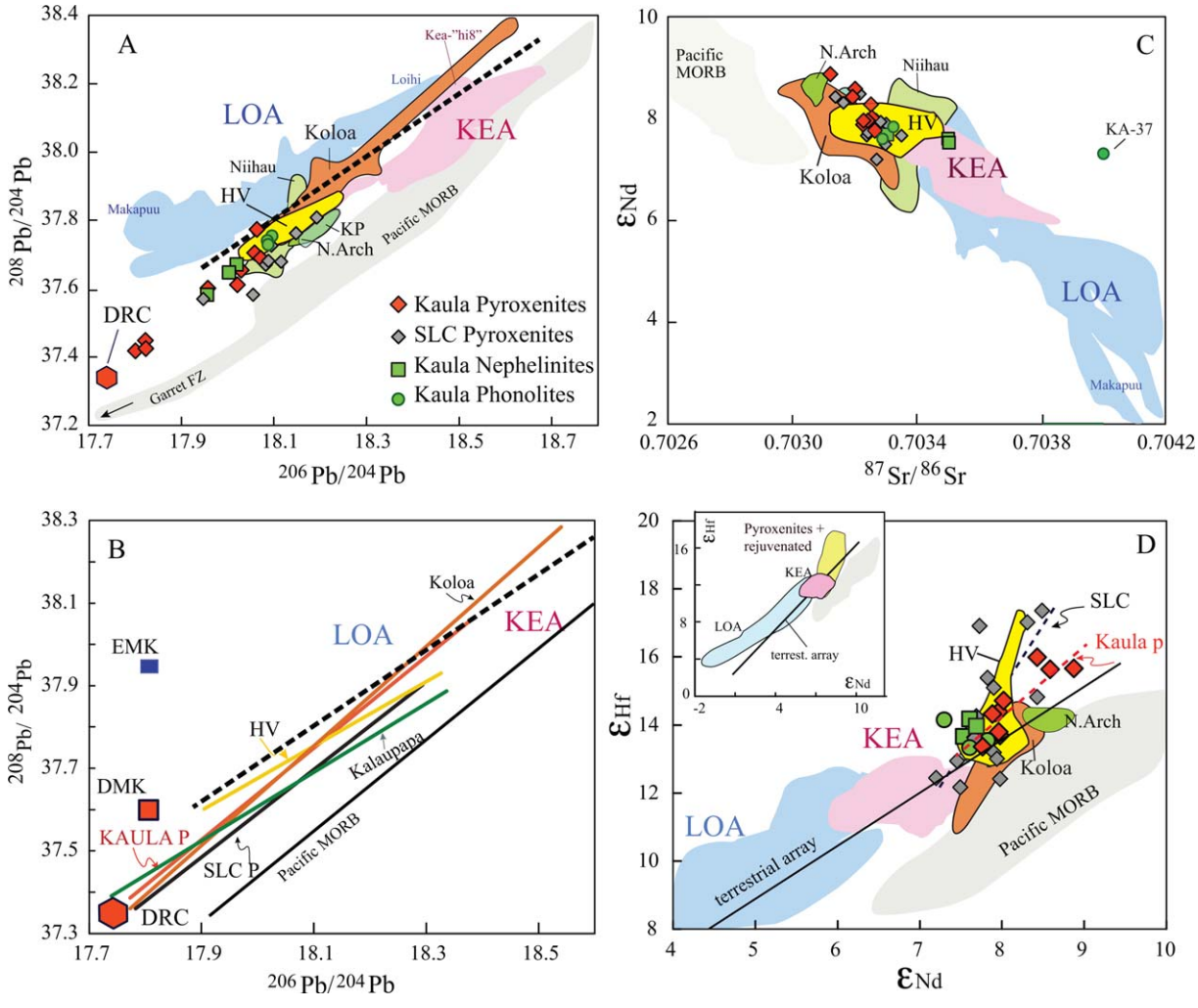

Figure 5. Continued

high temperatures may then reflect transient heating and reequilibration at shallower levels, perhaps during ascent from the mantle. In either case, the Kaula pyroxenites are considerably hotter than the calculated 90–100 Ma oceanic geotherm (Figure 6), the estimated age of the lithosphere under the Hawaiian islands based on the 110Ma age of ODP site 843 SW of Oahu [*Waggoner*, 1993] and ocean floor age reconstructions [*Müller et al*., 1997].

5.2. Crystal Fractionation Control on the Pyroxenite Compositions

5.2.1. Major Elements and REE

[26] The negative correlation between Na_2O and Mg# in the clinopyroxenes from the Kaula (and SLC) pyroxenites is generally consistent with magmatic fractionation. Figure 2a shows that progressive clinopyroxene fractionation from a parental magma similar to the most primitive Kaula nephelinites [*Garcia et al*., 1986] and Honolulu Volcanics [*Clague and Frey*, 1982] with Mg#∼64 to 67, and Na_2O ∼ 2.9 to 3.2 wt%, will create increasingly higher Na and Fe contents in the residual melt and crystallizing clinopyroxene that match well with the Kaula and SLC clinopyroxene Na_2O and Mg# systematics. The influence of cocrystalizing garnet is limited as Na is also incompatible in garnet. The negative Mg# versus Al_2O_3 correlation is also consistent with such a model (Figure 2b), however the larger range of Al_2O_3 at a given Mg# likely reflects additional variation in the Al contents of the parent melt and possibly the crystallization of garnet where Al is compatible.

[27] The Nd/Yb ratios in the Kaula and SLC clinopyroxenes, taken as a proxy for LREE/HREE fractionation, increase with decreasing Mg# (Figure 7). Ytterbium is more compatible than Nd in clinopyroxene, and clinopyroxene fractionation

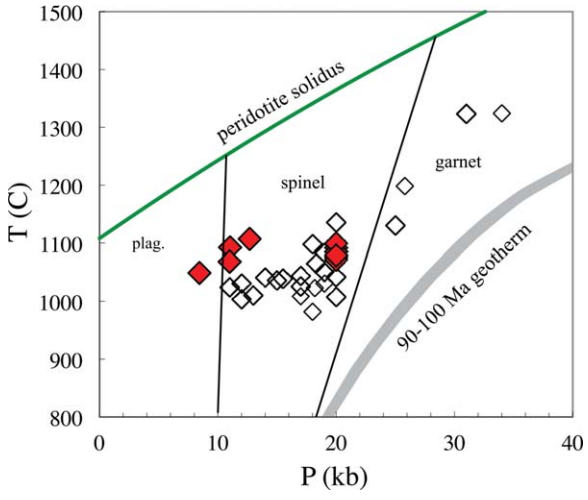

Figure 6. Pressure-temperature systematics of the Kaula pyroxenites, compared to the SLC pyroxenites [*Bizimis et al*., 2005] and the oceanic geotherm calculated for the 90–100 Ma old lithosphere. Temperatures are calculated with the two pyroxene thermometer and the BK barometer from *Brey and Köhler* [1990]. Dry peridotite solidus from *Hirschmann* [2000]. The stability fields for plagioclase, spinel and garnet peridotites are shown schematically. The geotherm is calculated by the half space cooling model, using a mantle temperature of 1300°C and thermal diffusivity of 10^{-6} m^2 s^{-1}.

will lead to residual melts with increasing Nd/Yb and decreasing Mg# (Figure 7). Garnet crystallization together with clinopyroxene will even further fractionate Nd/Yb in the residual melt. Allowing for variable Nd/Yb in the starting melt composition ($Nb/Yb_{(ch.norm)}$~12 to 36, within the range of Kaula lavas and Honolulu Volcanics [*Garcia et al*., 1986; *Yang et al*., 2003], fractional crystallization of a pyroxenitic mineralogy with a range of clinopyroxene to garnet ratios can reproduce the observed Kaula and SLC cpx Nb/Yb versus Mg# systematics (Figure 7). Some Kaula samples are best fit with a lower D^{Yb}_{bulk} than the SLC pyroxenites which implies less garnet in the crystallizing Kaula mineral assemblage, qualitatively consistent with the overall lower modal abundance of garnet in the Kaula pyroxenites compared to the SLC.

[28] In summary, the major and trace element systematics suggest that the Kaula pyroxenites formed within the lithosphere (<100 km) as crystallization products of parental melts similar to erupted rejuvenated magmas, in agreement with their generally similar isotope systematics. We emphasize that there are no obvious correlations between major or trace element systematics and

Figure 5. Isotope compositions of the Kaula lavas, pyroxenites and SLC pyroxenites, compared with Hawaiian shield and rejuvenated lavas and Pacific MORB. (a) $^{206}Pb/^{204}Pb$ versus $^{208}Pb/^{204}Pb$. All data has been normalized to the same NIST 987 value as the Kaula samples for direct comparison. The LOA and KEA shield stage lavas divide (dashed line) is from *Abouchami et al*. [2005]. (b) Regression lines through the $^{206}Pb/^{204}Pb$ versus $^{208}Pb/^{204}Pb$ ratios of rejuvenated lavas and pyroxenites. Slopes of the regression lines are given in the text. The Koloa field includes the Koloa Volcanics and Kauai postshield lavas. The Koloa Volcanics and Kaula lavas and pyroxenites form an array that crosses into the LOA side of the diagram and extends to the "KEA-hi8" or Loihi compositions. The Honolulu Volcanics and Kalaupapa Volcanics have shallower slopes and remain on the KEA side of the LOA-KEA divide (see text for discussion). The proposed composition of DRC is shown as a red hexagon. DMK and EMK compositions are from *Tanaka et al*. [2008]. (c) $^{87}Sr/^{86}Sr$ versus ε_{Nd} systematics. (d) ε_{Nd} versus ε_{Hf} systematics. Terrestrial array from *Vervoort et al*. [2011]. All Hf data are normalized to the JMC 475 value of $^{176}Hf/^{177}Hf = 0.282160$. Dashed lines are regression lines through the Kaula and SLC pyroxenites, with slopes of 2.1 and 3.6, respectively, steeper than the terrestrial array (note that the one SLC pyroxenite that plots just above the North Arch field is not included in the SLC regression). Abbreviations: KP: Kalaupapa. N.Arch: North Arch. HV: Honolulu Volcanics. DRC: depleted rejuvenated component. Data sources: Kaula lavas and xenoliths from this study. SLC pyroxenites: this study, [*Bizimis et al*., 2005]. Other rejuvenated lavas: Niihau: [*Dixon et al*., 2008]. Koloa Volcanics (Kauai): [*Reiners and Nelson*, 1998; *Lassiter et al*., 2000; *Garcia et al*., 2010]. Honolulu Volcanics (Koolau): [*Stille et al*., 1983; *Lassiter et al*., 2000; *Frey et al*., 2005; *Fekiacova et al*., 2007]. North Arch: [*Frey et al*., 2000]. Kalaupapa (East Molokai): [*Xu et al*., 2005]. Hualalai postshield lavas [*Hanano et al*., 2010]; KEA-trend volcanoes: West Maui: [*Gaffney et al*., 2004], Kohala: [*Hanano et al*., 2010]; Kilauea: [*Blichert-Toft et al*., 1999; *Abouchami et al*., 2005]. Mauna Kea: [*Blichert-Toft et al*., 2003; *Eisele et al*., 2003; *Abouchami et al*., 2005; *Bryce et al*., 2005; *Blichert-Toft and Albarède*, 2009; *Hanano et al*., 2010]. LOA trend volcanoes: Lanai [*Abouchami et al*., 2005; *Gaffney et al*., 2005], West Kaena: [*Garcia et al*., 2010]. Kahoolawe: [*Leeman et al*., 1994; *Blichert-Toft et al*., 1999; *Huang et al*., 2005]. Mauna Loa: [*Blichert-Toft et al*., 2003; *Wanless et al*., 2006; *Marske et al*., 2007; *Tanaka et al*., 2008; *Weis et al*., 2011]. Koolau: [*Stille et al*., 1983; *Abouchami et al*., 2005; *Salters et al*., 2006; *Fekiacova et al*., 2007; *Tanaka et al*., 2008; *Salters et al*., 2011]; Loihi: [*Staudigel et al*., 1984; *Blichert-Toft et al*., 1999; *Abouchami et al*., 2005]. Pacific MORB and Garret Fracture Zone [*White et al*., 1987; *Prinzhofer et al*., 1989; *Mahoney et al*., 1994; *Cousens et al*., 1995; *Castillo et al*., 1998; *Nowell et al*., 1998; *Salters and White*, 1998; *Niu et al*., 1999; *Regelous et al*., 1999; *Wendt et al*., 1999; *Castillo et al*., 2000; *Chauvel and Blichert-Toft*, 2001; *Sims et al*., 2003; *Salters et al*., 2011].

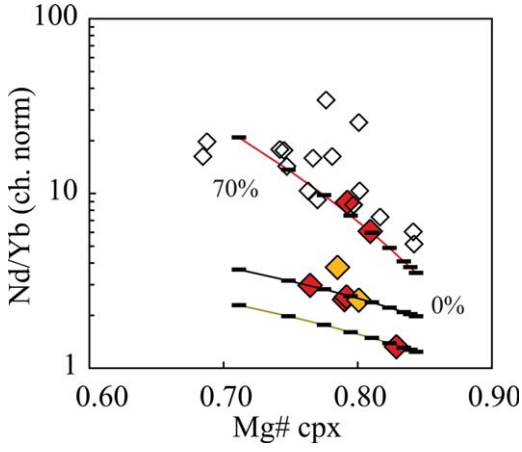

Figure 7. Chondrite normalized Nd/Yb versus Mg# in clinopyroxenes from the Kaula and SLC pyroxenites [*Bizimis et al*., 2005]. Symbols as in Figure 2. Note the increase in Nd/Yb ratio with increasing differentiation (decreasing Mg# in cpx). Curves show the evolution of cpx compositions in equilibrium with a fractionating melt, with a starting composition: Mg#=0.64 and $Nd/Yb_{(ch.\ norm.)} = 36$ (top), 20 (middle), 12.5 (bottom), roughly in the range of the erupted Kaula and Honolulu Volcanics nephelinites. $K_D^{Fe/Mg}{}_{cpx/melt}=0.35$. Two sets of Yb partition coefficients are used assuming cpx:gt ratio of 60:40 and 90:10 respectively in the fractionating mineral assemblage: $D^{Yb}{}_{bulk}= 1.6$ (top), 0.58 (middle and bottom), $D^{Nd}{}_{bulk} = 0.07$ (top, middle and bottom). $D^{Yb}{}_{bulk}$ and $D^{Nd}{}_{bulk}$ are calculated using $D^{Yb}{}_{cpx} =0.27$, $D^{Yb}{}_{gt}=3.5$, $D^{Nd}{}_{cpx} =0.07$, $D^{Nd}{}_{gt}=0.07$, from coexisting garnet and cpx in experiment RD-1097-5 of *Salters et al*. [2002].

the isotope compositions in the Kaula pyroxenites. This suggests that any source heterogeneity reflected in the parental melt major and trace element composition has been obscured by the subsequent fractionation and crystallization of these rocks. Furthermore, the occurrence of garnet pyroxenite xenoliths at Kaula and SLC, some 300 km apart, suggest that high-pressure crystallization of rejuvenated-type magmas may be common beneath the Hawaiian chain, and perhaps in other OIB settings. This likely has implications for the rheology and seismic structure of the oceanic lithosphere, as well as the composition of the recycled oceanic lithosphere, but such discussion is beyond the scope of this paper.

5.3. Constraints on the Source of the Hawaiian Rejuvenated Volcanism

[29] The radiogenic Hf, Nd, and unradiogenic Sr and Pb isotope compositions of the Kaula nephelinites and pyroxenites are common in Hawaiian rejuvenated volcanism. Recycled oceanic crust has been invoked to explain the radiogenic Sr and unradiogenic Nd isotopes of the shield stage magmas [*Hauri*, 1996; *Huang and Frey*, 2005]. The isotopic compositions however suggest that the magmas parental to the Kaula pyroxenites did not contain a significant amount of recycled oceanic crust. It is also unlikely that they represent "secondary pyroxenites" formed as reaction products of a melt from such recycled oceanic crustal lithologies with peridotite [*Sobolev et al*., 2005].

[30] We note that SLC garnet pyroxenite NMNH-114954-28A from our study has exsolved orthopyroxene in garnet, inferred as pseudomorphs after majoritic garnet, which would indicate crystallization pressure >5 GPa [*Keshav and Sen*, 2001]. Sample NMNH-114954-20A has ilmenite exsolution in garnet, and is also thought to have crystallized at >5GPa [*Keshav and Sen*, 2001]. These two samples indicate crystallization deeper than the seismically imaged lithosphere in Hawaii (88±7 km) [*Priestley and Tillman*, 1999], and were thought to perhaps represent recycled oceanic crust in the plume [*Keshav and Sen*, 2001]. However, the radiogenic Nd and unradiogenic Sr isotopes of both samples reported here (Table 1) entirely overlap with other SLC pyroxenites and rejuvenated magmas, and lack the enriched isotope compositions of an eclogite or "secondary pyroxenite" invoked to explain the high silica concentrations of shield stage volcanism [*Hauri*, 1996; *Sobolev et al*., 2005]. The isotopic compositions inferred for the source of the shield stage lavas remain elusive in the pyroxenite population.

[31] There is no correlation between Lu/Hf versus $^{176}Hf/^{177}Hf$ and Sm/Nd versus $^{143}Nd/^{144}Nd$ ratios in the Kaula pyroxenite cpx. Similarly, no correlation was observed in the cpx-garnet and bulk rock Lu-Hf and Sm-Nd isotope systematics of the SLC pyroxenites [*Bizimis et al*., 2005] as well as their bulk Re-Os isotope systematics [*Sen et al*., 2011]. These data argue against these rocks having formed within the Pacific lithosphere at ~90 Ma ago at a mid oceanic ridge [e.g., *Lassiter et al*., 2000]. Therefore we conclude that the measured isotopic compositions in the Kaula and SLC pyroxenites reflect their initial isotopic compositions, and that these in turn reflect those of their mantle sources.

5.3.1. The Depleted Rejuvenated Component

[32] The Kaula nephelinites and pyroxenites and Hawaiian rejuvenated lava data delineate a "rejuvenated volcanism" array that extends to lower $^{208}Pb/^{204}Pb$ at a given $^{206}Pb/^{204}Pb$ than the LOA-trend lavas and has less radiogenic Pb

isotope ratios than KEA-trend shield lavas. The Kaula phonolites overlap this array. In $^{206}Pb/^{204}Pb$-$^{208}Pb/^{204}Pb$ space, the slopes defined by all pyroxenites and Kaula lavas are parallel, but offset to higher $^{208}Pb/^{204}Pb$ at a given $^{206}Pb/^{204}Pb$, compared to the Pacific MORB field (Figures 5a and 5b), which includes the Garret Transform fault lavas with highly unradiogenic Pb isotopes. This argues against involvement of a Pacific MORB mantle source in the Kaula and the SLC pyroxenites source, in agreement with the conclusions reached for other rejuvenated lava sources [*Fekiacova et al.*, 2007; *Garcia et al.*, 2010]. Extension of the arrays defined by the Kaula, Koloa, SLC pyroxenites and Kalaupapa Volcanics arrays toward unradiogenic $^{208}Pb/^{204}Pb$-$^{206}Pb/^{204}Pb$ converge around $^{208}Pb/^{204}Pb = 37.35 \pm 0.05$, $^{206}Pb/^{204}Pb = 17.75 \pm 0.05$ (Figure 5b). This convergence suggests that this composition may represent a common end-member component in the source of rejuvenated volcanism. Following *Fekiacova et al.* [2007] we call this component the Depleted Rejuvenated Component (DRC). By defining the DRC in $^{206}Pb/^{204}Pb$-$^{208}Pb/^{204}Pb$ isotope space we can use the correlations between Pb isotopes and the other isotope systems to define its Hf, Nd, Sr isotope compositions.

[33] In εNd-$^{208}Pb/^{204}Pb$ isotope space (Figure 8a), the coupled unradiogenic Pb and radiogenic Nd isotope compositions of the rejuvenated array, currently best represented by the Kaula pyroxenites, constrain the Nd isotope composition of DRC at ε_{Nd} ~9 to 10. In a similar fashion, the Sr-Nd isotope systematics for the Kaula and SLC pyroxenites suggest $^{87}Sr/^{88}Sr < 0.70305$ for the DRC.

[34] The different slopes of the SLC and Kaula pyroxenites in ε_{Hf}-ε_{Nd} space (Figure 5d) make it difficult to define a single Hf isotope composition for DRC. This is also evident in Hf-Pb isotope space (Figure 8b) where some SLC pyroxenite [*Bizimis et al.*, 2005] and Honolulu Volcanics data [*Stille et al.*, 1983] extend to more radiogenic ε_{Hf} at a given $^{206}Pb/^{204}Pb$ than the Kaula lavas and pyroxenites. Nevertheless, the ε_{Hf}-$^{206}Pb/^{204}Pb$ systematics of the Kaula pyroxenites are highly correlated, and together with the Kaula lavas, Koloa Volcanics and most of the Honolulu Volcanics and SLC pyroxenites constrain the DRC to have $\varepsilon_{Hf} = 16$–17 at $^{206}Pb/^{204}Pb = 17.75$.

[35] The radiogenic Nd, Hf and unradiogenic Sr, Pb isotope compositions of DRC suggest a source with relatively low, time-integrated Rb/Sr, U/Pb, Th/Pb and high Lu/Hf, Sm/Nd parent/daughter ratios. These ratios are qualitatively consistent with the partitioning of these elements in the residual mantle during peridotite melting [*Salters et al.*, 2002]. The DRC isotope composition is therefore consistent with a peridotite that is residual after an ancient partial melt extraction event. The relatively radiogenic Hf at a given Nd isotope compositions of the SLC pyroxenites have been explained by mixing between plume (KEA-type) melts and those from an ancient (e.g. >1Ga)

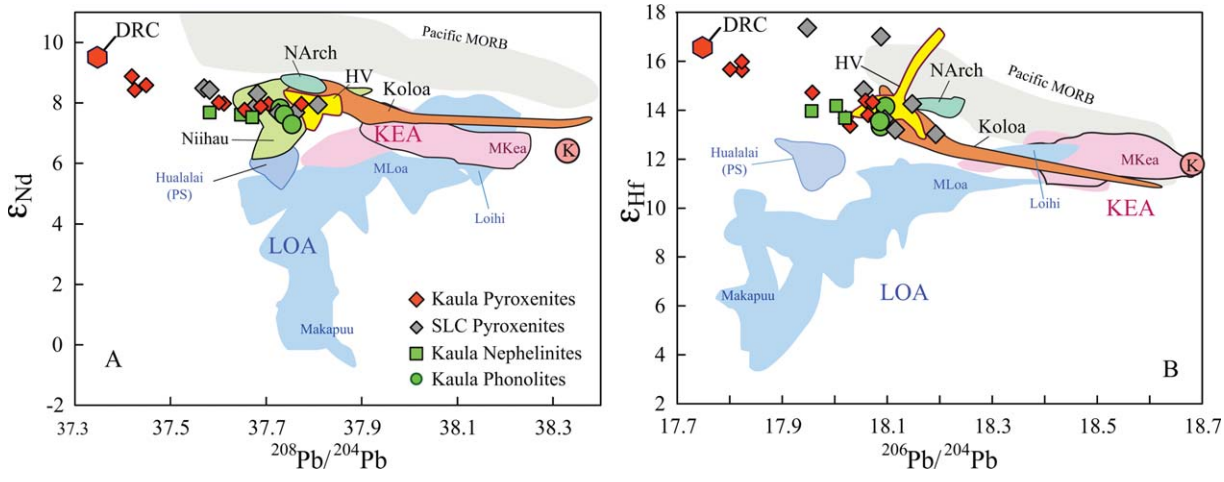

Figure 8. (a) ε_{Nd} versus $^{208}Pb/^{204}Pb$ and (b) ε_{Hf} versus $^{206}Pb/^{204}Pb$ isotope systematics of the Kaula lavas, pyroxenites and SLC pyroxenites compared to other rejuvenated and shield stage Hawaiian lavas. Data and abbreviations as in Figure 5. The proposed composition of DRC is shown as a red hexagon. Circle with "K" shows the composition of the KEA end-member proposed here. The fields for the Mauna Kea lavas and Hualalai postshield lavas are outlined to illustrate the slightly negative slope of the Mauna Kea compositions in Figure 8a, and the offset of the Hualalai compositions toward the DRC in both plots.

depleted mantle [*Bizimis et al*., 2005]. Peridotites with extremely radiogenic Hf and unradiogenic Os isotopic compositions in Oahu and Kauai were explained as reflecting an ancient depleted recycled mantle lithosphere within the Hawaiian plume [*Bizimis et al*., 2004; *Bizimis et al*., 2007; *Bizimis et al*., 2008]. An ancient depleted lithosphere has also been invoked in the source of the Koolau shield lavas [*Salters et al*., 2006], and is a long-lived source feature of the Hawaiian-Emperor Chain [*Frey et al*., 2005]. The above evidence favor an origin of the DRC as an ancient depleted mantle that is part of the plume. Note, however, that the elevated incompatible element concentrations of the rejuvenated Hawaiian alkalic lavas [*Clague and Frey*, 1982; *Yang et al*., 2003; *Garcia et al*., 2010] are hard to reconcile with direct melting of a depleted peridotite. Instead, several studies suggested that metasomatic enrichment of a depleted source shortly before melting is required [*Roden et al*., 1984; *Salters and Zindler*, 1995; *Reiners and Nelson*, 1998; *Yang et al*., 2003; *Dixon et al*., 2008].

5.3.2. The Enriched Components in the Rejuvenated Source

[36] At its radiogenic Pb isotope extension, the array defined by the Kaula lavas and pyroxenites and the Koloa Volcanics crosses the LOA-KEA divide into the LOA region of the $^{206}Pb/^{204}Pb$ versus $^{208}Pb/^{204}Pb$ plot (Figures 5a and 5b). In contrast, other rejuvenated lavas (Honolulu Volcanics, Kalaupapa) have shallower slopes and remain on the KEA side of the LOA-KEA divide (Figure 5b). To a first approximation, this suggests the contribution of both LOA and KEA type sources to the rejuvenated volcanism. In detail however, this Kaula-Koloa Volcanics array points to a "Loihi" or "Kea-hi8" [*Abouchami et al*., 2005] type composition with relatively radiogenic $^{208}Pb/^{204}Pb$ at a given $^{206}Pb/^{204}Pb$, and not to the more isotopically extreme LOA sources of the Makapuu (Koolau) Lanai, or Kahoolawe shield lavas with relatively unradiogenic $^{208}Pb/^{204}Pb$ (Figures 5a and 5b). This is further evident in ε_{Nd}-$^{208}Pb/^{204}Pb$ and ε_{Hf}-$^{206}Pb/^{204}Pb$ space (Figure 8) where there appears to be a compositional continuity from the DRC, through the rejuvenated magmas, toward the KEA and/or Loihi type compositions only, and not toward the other LOA type compositions. It is unclear whether *both* Loihi and KEA type sources contribute to rejuvenated magmas, or there is simply a large enough variability in the Pb isotope compositions of the KEA source alone to explain the radiogenic Pb isotope variability of the rejuvenated magmas.

[37] In this context, the previously proposed KEA end-member isotope composition with ε_{Hf} ~14, ε_{Nd} ~9 at $^{206}Pb/^{204}Pb$ ~ 18.8 and $^{208}Pb/^{204}Pb$ ~38.35 [*Tanaka et al*., 2008] appears too radiogenic in Nd and Hf isotopes and falls significantly off the trend defined by the KEA lavas in ε_{Nd} versus $^{208}Pb/^{204}Pb$ and ε_{Hf} versus $^{206}Pb/^{204}Pb$ space (Figures 8a and 8b). In particular, the slightly negative slope defined by the Mauna Kea HSDP lavas in ε_{Nd} versus $^{208}Pb/^{204}Pb$ space requires that the KEA end-member has less radiogenic Nd isotope composition than DRC. Based on the trends in Figures 8a and 8b, we suggest that the KEA end-member should be revised to $\varepsilon_{Nd} = 6–7$, $\varepsilon_{Hf} = 11–12$, with $^{87}Sr/^{86}Sr = 0.7035–0.7036$, $^{206}Pb/^{204}Pb = 18.7–18.8$, $^{208}Pb/^{204}Pb = 38.3–38.4$ similar to values proposed by *Tanaka et al*. [2008].

6. Implications for the Geochemical Structure of the Hawaiian Plume

[38] The DRC proposed here allows us to reinterpret some previously proposed components for the Hawaiian volcanism. The Depleted Makapuu Koolau (DMK) component has been invoked to explain the unradiogenic Pb compositions of the Koolau shield stage and rejuvenated Honolulu Volcanics [*Tanaka et al*., 2008]. In $^{206}Pb/^{204}Pb$-$^{208}Pb/^{204}Pb$ space (Figure 5b), DMK falls between DRC and the Enriched Makapuu Koolau component of *Tanaka et al*. [2008]. In this case, the unradiogenic Pb compositions of the Honolulu Volcanics can be explained by mixing between DRC and the Enriched Makapuu Koolau end-member (Figure 5b) and DMK is not required as a separate entity. If correct, this mixing relationship also implies a contribution from a LOA-type source (Enriched Makapuu Koolau) to the rejuvenated volcanism in Koolau, which is best seen in the Pb isotope systematics of Honolulu Volcanics (Figure 5b).

[39] The slightly negative slope defined by the Mauna Kea lavas in ε_{Nd}-$^{208}Pb/^{204}Pb$ space (Figure 8a) toward the DRC and away from the low ε_{Nd}-low$^{208}Pb/^{204}Pb$ ratios of the extreme LOA compositions, also implies that the DRC may also contribute to the KEA shield / post shield stage volcanism. A mixed DRC-KEA source appears to also contribute to some LOA shield and postshield volcanoes. For example, the so-called "Kalihi" component with $^{206}Pb/^{204}Pb = \sim 18.3$, $^{208}Pb/^{204}Pb$ ~37.9 invoked to be common in the source of the rejuvenated Honolulu Volcanics and the KSDP (Koolau) shield lavas [*Fekiacova et al*., 2007], is

internal to the DRC-KEA compositional range and therefore may be a mixture of these two as opposed to a physically distinct entity in the plume. Moreover, the Hualalai postshield lavas [*Hanano et al*., 2010], a LOA trend volcano, show a shift from the LOA shield compositions toward the DRC in both ε_{Nd} versus $^{208}Pb/^{204}Pb$ and ε_{Hf} versus $^{206}Pb/^{204}Pb$ space (Figures 8a and 8b). Finally, a contribution of a depleted component, similar to that sampled during rejuvenated volcanism has been proposed for the Kauai shield lavas [*Mukhopadhyay et al*., 2003]. The above observations suggest that KEA and DRC may be locally mixed and that DRC may contribute to LOA shield (e.g., KSDP) and postshield (e.g., Hualalai) volcano sources.

[40] The DRC is recognized in the compositions of xenoliths and lavas erupted in the last ~4.2 Ma along 300 km of the Hawaiian Island chain (Kauai-Kaula to East Molokai). The compositions of the ~76 to 81 Ma lavas from Detroit Seamount along the Emperor Seamount chain [*Frey et al*., 2005] are also consistent with the DRC composition proposed here. These observations are consistent with the DRC being a long-lived feature of the Hawaiian plume, rather than a local component fortuitously incorporated in the source of the Kaula parental magmas. The increased proportion of the DRC in the rejuvenated rather than the shield stage lavas can be explained by melting of a heterogeneous plume, where the more fertile and isotopically enriched components preferentially melt and dominate the chemistry of the voluminous shield lavas. Exhaustion of the enriched components after the shield stage melting event leaves a residual plume mantle with an increased proportion of the more refractory DRC. This depleted plume source subsequently melts downstream from the plume center and at the edges of the Hawaiian swell, either due to a secondary melting zone [*Ribe and Christensen*, 1999], lithosphere flexing [*Bianco et al*., 2005], erosion of the lithosphere by the plume [*Li et al*., 2004; *Ballmer et al*., 2011], or some combination thereof [*Garcia et al*., 2010], leading to a higher proportion of DRC in the source of rejuvenated volcanism.

6.1. Rejuvenated Source Heterogeneity Across the Plume Track

[41] The rejuvenation stage lavas from Kaula, Niihau, Kauai, and North Arch volcanic field fall on a ~400 km transect that strikes approximately orthogonal to the Hawaiian Islands (Figure 1). The ages of rejuvenated volcanism along this transect approximately overlap. Kaula nephelinites and pyroxenite xenoliths are younger than 1.8 Ma. The Niihau lavas erupted between 2.5 and 0.3 Ma [*Clague and Dalrymple*, 1987; *Moore and Clague*, 2004; *Sherrod et al*., 2007]. The Koloa Volcanics erupted between 2.6 to 0.15Ma [*Garcia et al*., 2010]. The North Arch lavas erupted between 1.15 and 0.5 Ma based on Mn-coating thickness [*Moore and Clague*, 2004]. Therefore, the compositions of these lavas provide a snapshot of the geochemical variability of the rejuvenated source across the plume track. There is a systematic increase from southwest to northeast in $^{208}Pb/^{204}Pb$ ratios for Kaula Niihau, and Kauai rejuvenated lavas, and then a slight decrease for North Arch lavas (Figure 9a). These trends are less apparent in Nd isotopes (Figure 9b). However, the peripheral Kaula pyroxenites and North Arch lavas have, on average, more radiogenic Nd isotopes ($^{143}Nd/^{144}Nd = 0.513056 \pm 19$ and 0.513076 ± 12, 1 standard deviation, respectively) than the Kauai and Niihau rejuvenated lavas ($^{143}Nd/^{144}Nd = 0.513037 \pm 29$ and 0.513039 ± 36, respectively). Similarly Kaula pyroxenites and North Arch lavas have, on average, more radiogenic Hf isotope compositions ($^{176}Hf/^{177}Hf = 0.283198 \pm 27$ and 0.283183 ± 6 respectively) than the Koloa Volcanics ($^{176}Hf/^{177}Hf = 0.283143 \pm 29$). The Sr isotope compositions are more scattered and do not allow for a meaningful comparison. The limited isotope data from the North Arch volcanic field notwithstanding, the Pb, Nd, Hf isotope patterns imply a larger contribution of the DRC to the rejuvenated magmas at the edges of the plume, than along the plume track.

[42] The addition of rejuvenated magma data from other locations along the plume track, for example the West Kaena alkali lavas erupted at 1.39–0.38 Ma [*Greene et al*., 2010], the Oahu Honolulu Volcanics at 0.8–0.1 Ma [*Ozawa et al*., 2005] and SLC pyroxenites, does not significantly change the observed patterns. It does however add more complexity to the interpretation as it also compares the Kaula-North Arch transect with lavas from along the plume track closer to the present day plume center. Plume material is thought to disperse downstream from the plume center [*Ribe and Christensen*, 1999; *Farnetani and Hofmann*, 2010; *Ballmer et al*., 2011]. However it is unclear how it is distributed with distance from the plume center. To avoid this complexity, here we only discuss the isotopic gradients across the plume track from Kaula to North Arch.

[43] One interpretation for the larger proportion of the DRC at the periphery of the plume is that it represents entrained mantle [*Fekiacova et al*.,

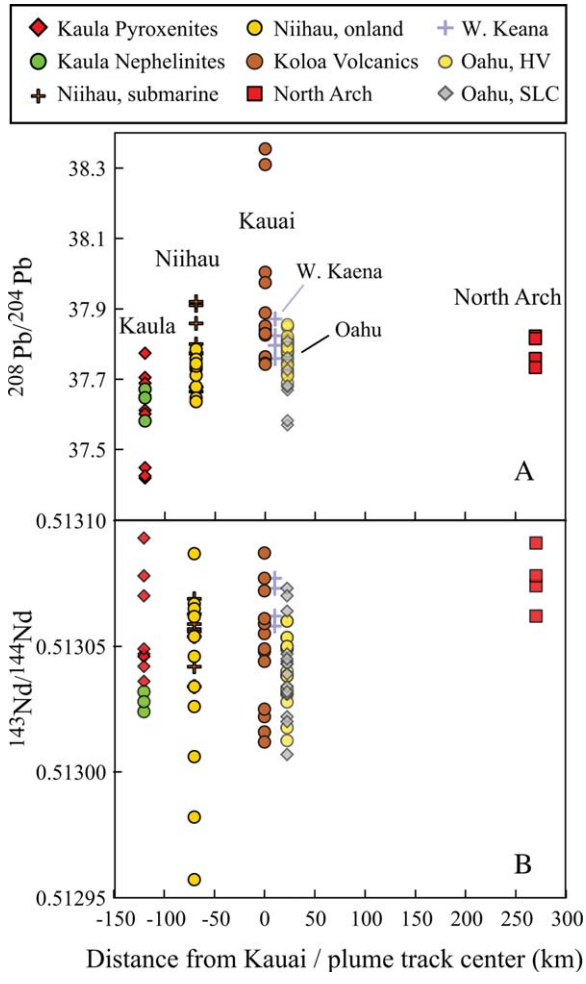

Figure 9. (a) $^{208}Pb/^{204}Pb$, and (b) $^{143}Nd/^{144}Nd$ isotope variability of rejuvenated lavas from Kaula, Niihau, Kauai, North Arch with distance across the center of the plume track. Distances are calculated from the center of Kauai, taken here as the center of the plume track, to the center of the islands and the coordinates of the plotted North Arch samples [*Frey et al*., 2000]. Data sources as in Figure 5. The Niihau samples are separated into submarine and onland for clarity. Kaula and North Arch at the periphery of the plume have less radiogenic Pb and more radiogenic Nd isotope ratios than the Kauai and Niihau rejuvenated lavas closer to the center. The Oahu (SLC and Honolulu Volcanics) and West Kaena rejuvenated lavas are shown for comparison with lighter colors (see text for discussion).

2007; *Ballmer et al*., 2011] that is similar to, but compositionally distinct from, the source of Pacific MORB. In this scenario the enriched plume component is not entirely exhausted during the shield stage, and contributes to the rejuvenated volcanism downstream from the plume center (e.g., Kauai), leading to less radiogenic Nd, Hf and more radiogenic Pb isotopes than the peripheral (Kaula, North Arch) rejuvenated volcanism. Alternatively, if there is no significant upper mantle entrainment during plume upwelling [*Farnetani et al*., 2002] then the DRC might be traced to the source of the plume (perhaps the core mantle boundary) together with the LOA and KEA components [*Farnetani and Hofmann*, 2010; *Farnetani et al*., 2012]. The isotope systematics would then require a greater proportion of the enriched components (e.g., LOA, KEA) in the plume center than in the periphery, and proportionally larger contribution from the enriched plume core to the rejuvenated volcanism downstream from the plume center (e.g., Kauai) than the off-axis volcanism (Kaula, North Arch). In either scenario however, there is evidence for a greater proportion of the DRC in the rejuvenated magma source at the periphery of the plume than downstream from the plume center. Additional data from the off-axis rejuvenated volcanism could further test this hypothesis and may help distinguish whether the DRC is entrained mantle versus a component integral to the Hawaiian plume.

7. Conclusions

[44] 1. The Kaula pyroxenites formed as cumulates within the Pacific lithosphere from melts geochemically similar to the alkalic rejuvenated lavas erupted at Kaula volcano. The broadly similar major, trace element and isotope compositions of the Kaula and SLC pyroxenite xenoliths that erupted some 300 km apart suggest that such high pressure (>20 kb) crystal fractionates might be a common byproduct of Hawaiian volcanism, and perhaps oceanic island volcanism elsewhere.

[45] 2. Nephelinites, phonolites and garnet pyroxenite xenoliths from Kaula Island have radiogenic Hf, Nd, and unradiogenic Sr isotope compositions, consistent with a time-integrated depleted peridotitic source. The Pb isotope compositions of the Kaula pyroxenites, nephelinites and Salt Lake Crater pyroxenites extend to the lowest $^{208}Pb/^{204}Pb$ reported in Hawaiian volcanism. These new data allow the composition of the isotopically depleted end-member component of the rejuvenated volcanism (DRC) to be redefined as $^{208}Pb/^{204}Pb = 37.35 \pm 0.05$, $^{206}Pb/^{204}Pb = 17.75 \pm 0.03$, $\varepsilon_{Nd} = 9$–10, $\varepsilon_{Hf} = 16$–17 and $^{87}Sr/^{88}Sr < 0.70305$. The rejuvenated magma compositions do not trend toward the Pacific MORB compositions, suggesting that DRC is distinct from the source of Pacific MORB. Based on the isotope systematics of the rejuvenated and KEA shield lavas we also propose a refined composition for the KEA end-member

at $\varepsilon_{Nd} = 6–7$, $\varepsilon_{Hf} = 11–12$, with $^{87}Sr/^{86}Sr = 0.7035–0.7036$, $^{206}Pb/^{204}Pb = 18.7–18.8$, $^{208}Pb/^{204}Pb = 38.3–38.4$.

[46] 3. The DRC is recognized in the compositions of xenoliths and lavas erupted in the last ~4.2 Ma and >300 km apart along the Hawaiian Island chain. The isotopic continuum between KEA shield and rejuvenated magmas suggests a close spatial association between KEA and DRC. The DRC is also recognized in the compositions of the LOA-trend Koolau shield and Hualalai postshield lavas. The compositions of the ~76 to 81 Ma Detroit Seamount lavas from the Emperor Seamount chain [*Frey et al*., 2005] are also consistent with the DRC composition proposed here. All these observations are consistent with the DRC being a long-lived component of the Hawaiian plume.

[47] 4. The Kaula pyroxenites and North Arch rejuvenated lavas at the periphery of the plume have on average less radiogenic Pb and more radiogenic Nd and Hf isotope compositions than Kauai and Niihau rejuvenated lavas near the center of the plume track. This suggests a larger proportion of the depleted component at the periphery of the plume than along the Island chain during rejuvenated volcanism.

[48] These results indicate that the DRC, which is dominantly sampled during rejuvenated volcanism and currently best represented by the Kaula pyroxenites, is also widely available and contributes to the KEA shield, and (at least in some instances) LOA shield volcanism. This depleted component appears to be dispersed within the plume, but with a larger proportion at the periphery than the center.

Acknowledgments

[49] We would like to thank James Day, Fred Frey and Al Hofmann for their in-depth comments and suggestions that significantly improved this presentation, and Janne Blichert-Toft for editorial handling. Thanks to Shichun Huang for many discussions on Hawaiian volcanism. Many thanks to Elizabeth Bair and Carl Frisby at USC for help with the analyses. This work was supported by the National Science Foundation grants OCE-0622827, OCE-0820723, OCE-1129280 to MB and EAR-0510482 to MG.

References

Abouchami, W., A. W. Hofmann, S. J. G. Galer, F. A. Frey, J. Eisele, and M. Feigenson (2005), Lead isotopes reveal bilateral asymmetry and vertical continuity in the Hawaiian mantle plume, *Nature*, *434*, 851–856.

Anders, E., and N. Grevesse (1989), Abundances of the elements: Meteoritic and solar, *Geochim. Cosmochim. Acta*, *53*, 197–214.

Ballmer, M. D., G. Ito, J. van Hunen, and P. Tackley (2011), Spatial and temporal variability in Hawaiian hotspot volcanism induced by small-scale convection, *Nat. Geosci.*, *4*, 457–460, doi:10.1038/ngeo1187.

Beeson, M. H., and E. D. Jackson (1970), Origin of garnet pyroxenite xenoliths at Salt Lake crater, Oahu, Hawaii, *Mineral. Soc. Am. Spec. Pap.*, *3*, 95–112.

Bianco, T. A., G. Ito, J. M. Becker, and M. O. Garcia (2005), Secondary Hawaiian volcanism formed by flexural arch decompression, *Geochem. Geophys. Geosyst.*, *6*, Q08009, doi:10.1029/2005GC000945.

Bizimis, M., G. Sen and V. J. M. Salters (2004), Hf-Nd isotope decoupling in the oceanic lithosphere: Constraints from spinel peridotites from Oahu, Hawaii, *Earth Planet. Sci. Lett.*, *217*, 43–58.

Bizimis, M., G. Sen, V. J. M. Salters and S. Keshav (2005), Hf-Nd-Sr isotope systematics of garnet pyroxenites from Salt Lake Crater, Oahu, Hawaii: Evidence for a depleted component in Hawaiian volcanism, *Geochim. Cosmochim. Acta*, *69*, 2629–2646.

Bizimis, M., V. J. M. Salters, S. Huang, and D. Clague (2008), 1. Ga old plume-derived peridotite xenoliths from Kauai, Hawaii, *Geochim. Cosmochim. Acta*, *72*(12), A94.

Bizimis, M., M. Griselin, J. C. Lassiter, V. J. M. Salters, and G. Sen (2007), Ancient recycled mantle lithosphere in the Hawaiian plume: Osmium-Hafnium isotopic evidence from peridotite mantle xenoliths, *Earth Planet. Sci. Lett.*, *257*, 259–273.

Blichert-Toft, J., and F. Albarède (2009), Mixing of isotopic heterogeneities in the Mauna Kea plume conduit, *Earth Planet. Sci. Lett.*, *282*(1–4), 190–200, doi:10.1016/j.epsl.2009.03.015.

Blichert-Toft, J., F. A. Frey, and F. Albarède (1999), Hf isotope evidence for pelagic sediments in the source of Hawaiian Basalts, *Science*, *285*, 879–882.

Blichert-Toft, J., D. Weis, C. Maerschalk, A. Agranier, and F. Albarède (2003), Hawaiian hot spot dynamics as inferred from Hf and Pb isotope evolution of Mauna Kea volcano, *Geochem. Geophys. Geosyst.*, *4*(2), 8704, doi:10.1029/2002GC000340.

Brey, G. P., and T. Köhler (1990), Geothermobarometry in four phase lherzolites: II. New thermobarometers and practical assessment of existing thermobarometers, *J. Petrol.*, *31*, 1353–1378.

Bryce, J. G., D. J. DePaolo, and J. C. Lassiter (2005), Geochemical structure of the Hawaiian plume: Sr, Nd, and Os isotopes in the 2.8 km HSDP-2 section of Mauna Kea volcano, *Geochem. Geophys. Geosyst.*, *6*, Q09G18, doi:10.1029/2004GC000809.

Castillo, P. R., J. H. Natland, Y. L. Niu, and P. F. Lonsdale (1998), Sr, Nd and Pb isotopic variation along the Pacific-Antarctic risecrest, 53–57 degrees S: Implications for the composition and dynamics of the South Pacific upper mantle, *Earth Planet. Sci. Lett.*, *154*(1-4), 109–125.

Castillo, P. R., E. Klein, J. Bender, C. Langmuir, S. Shirey, R. Batiza, and W. White (2000), Petrology and Sr, Nd, and Pb isotope geochemistry of mid-ocean ridge basalt glasses from the 11 degrees 45' N to 15 degrees 00' N segment of the East Pacific Rise, *Geochem. Geophys. Geosyst.*, *1*, 1011, doi:10.1029/1999GC000024.

Chauvel, C., and J. Blichert-Toft (2001), A hafnium isotope and trace element perspective on melting of the depleted mantle, *Earth Planet. Sci. Lett.*, *190*(3-4), 137–151.

Clague, D. A., and F. A. Frey (1982), Petrology and trace element chemistry of the Honolulu volcanics, Oahu: Implication for the oceanic mantle below Hawaii, *J. Petrol*., *23*, 447–504.

Clague, D. A., and G. B. Dalrymple (1987), The Hawaiian-Emperor volcanic chain. Part I Geological evolution, in *Volcanism in Hawaii*, USGS Prof. Pap. 1350, edited by R. W. Decker, T. L. Wright, and P. H. Stauffer, pp. 5–54, Washington, D. C.

Clague, D. A., and J. E. Dixon (2000), Extrinsic controls on the evolution of Hawaiian ocean island volcanoes, *Geochem. Geophys. Geosyst.*, *1,1010*, doi:10.1029/1999GC000023.

Clague, D. A., R. T. Holcomb, J. M. Sinton, R. S. Detrick, and M. E. Torresan (1990), Plicocene and Pleistocene alkalic flood basalts on the seafloor north of the Hawaiian islands, *Earth Planet. Sci. Lett.*, *98*, 175–191.

Cousens, B. L., J. F. Allan, M. I. Leybourne, R. L. Chase, and N. Vanwagoner (1995), Mixing of magmas from enriched and depleted mantle sources the Northeast Pacific—West-Valley Segment, Juan-De-Fuca Ridge, *Contrib. Mineral. Petrol*., *120*(3-4), 337–357.

DePaolo, D. J., J. G. Bryce, A. Dodson, D. L. Shuster, and M. B. Kennedy (2001), Isotopic evolution of Mauna Loa and the chemical structure of the Hawaiian plume, *Geochem. Geophys. Geosyst.*, *2*, 1044, doi:10.1029/2000GC000139.

Dixon, J., D. A. Clague, B. Cousens, M. L. Monsalve, and J. Uhl (2008), Carbonatite and silicate melt metasomatism of the mantle surrounding the Hawaiian plume: Evidence from volatiles, trace elements, and radiogenic isotopes in rejuvenated-stage lavas from Niihau, Hawaii, *Geochem. Geophys. Geosyst*., *9*, Q09005, doi:10.1029/2008GC002076.

Eisele, J., W. Abouchami, S. J. G. Galer, and A. W. Hofmann (2003), The 320 kyr Pb isotopee evolution of Mauna Kea lavas recorder in the HSDP-2 drill core, *Geochem. Geophys. Geosyst.*, *4*(5), 8710, doi:10.1029/2002GC000339.

Ellis, D., and D. Green (1979), An experimental study of the effect of Ca upon garnet-clinopyroxene Fe-Mg exchange equilibria, *Contrib. Mineral. Petrol.*, *71*, 13–22.

Farnetani, C. G., and A. W. Hofmann (2010), Dynamics and internal structure of the Hawaiian plume, *Earth Planet. Sci. Lett.*, *295*(1-2), 231–240.

Farnetani, C. G., B. Legras, and P. Tackley (2002), Mixing and deformation in mantle plumes, *Earth Planet. Sci. Lett.*, *196*, 1–15.

Farnetani, C. G., A. W. Hofmann, and C. Class (2012), How double volcanic chains sample geochemical anomalies from the lowermost mantle, *Earth Planet. Sci. Lett.*, *359–360*, 240–247, doi:10.1016/j.epsl.2012.09.057.

Fekiacova, Z., W. Abouchami, S. J. G. Galer, M. O. Garcia, and A. W. Hofmann (2007), Origin and temporal evolution of Ko'olau Volcano, Hawai'i: Inferences from isotope data on the Koolau Scientific Drilling Project (KSDP), the Honolulu Volcanics and ODP Site 843, *Earth Planet. Sci. Lett*., *261*(1-2), 65–83.

Frey, F. A. (1980), The origin of pyroxenite and garnet pyroxenites from Salt Lake Crater, Oahu, Hawaii: Trace element evidence, *Am. J. Sci*., *280A*, 427–449.

Frey, F. A., D. Clague, J. J. Mahoney, and J. M. Sinton (2000), Volcanism from the edge of the Hawaiian plume: Petrogenesis of submarine alkalic lavas from the North Arch Voclanic Field, *J. Petrol.*, *41*, 667–691.

Frey, F. A., S. Huang, J. Blichert-Toft, M. Regelous, and M. Boyet (2005), Origin of depleted components in basalt related to the Hawaiian Hotspot: Evidence from isotopic and Incompatible element ratios, *Geochem. Geophys. Geosyst.*, *6*, Q02L07, doi:10.1029/2004GC000757.

Frezzotti, M.-L., E. A. J. Burke, B. De Vivvo, B. Stefanini, and I. M. Villa (1992), Mantle fluids in pyroxenite nodules from Salt Lake crater (Oahu, Hawaii), *Eur. J. Mineral*., *4*, 1137–1153.

Gaffney, A. M., B. K. Nelson, and J. Blichert-Toft (2004), Geochemical constraints on the role of oceanic lithosphere in intra-volcano heterogeneity at West Maui, Hawaii, *J. Petrol*., *45*, 1663–1687.

Gaffney, A. M., B. K. Nelson, and J. Blichert-Toft (2005), Melting in the Hawaiian plume at 1–2 Ma as recorded at Maui Nui: The role of eclogite, peridotite, and source mixing, *Geochem. Geophys. Geosyst.*, *6*, Q10L11, doi:10.1029/2005GC000927.

Ganguly, J., W. Cheng, and M. Tirone (1996), Thermodynamics of aluminosilicate garnet solid solution: New experimental data, an optimized model, and thermometric applications, *Contrib. Mineral. Petrol.*, *126*, 137–151.

Garcia, M. O., and A. A. Presti (1987), Glass in garnet pyroxenite xenoliths from Kaula Island, Hawaii: Product of infiltration of host nephelinite, *Geology*, *15*, 904–906.

Garcia, M. O., F. A. Frey, and D. G. Grooms (1986), Petrology of volcanic rocks from Kaula Island, Hawaii, implications for the origin of Hawaiian phonolites, *Contrib. Mineral. Petrol.*, *94*, 461–471.

Garcia, M. O., et al. (2008), Widespread secondary volcanism around the northern Hawaiian Islands, *Eos Trans. AGU*, *59*(52), 542.

Garcia, M. O., L. Swinnard, D. Weis, A. R. Greene, T. Tagami, H. Sano, and C. E. Gandy (2010), Petrology, geochemistry and geochronology of Kaua'i lavas over 4·5 Myr: Implications for the origin of rejuvenated volcanism and the evolution of the Hawaiian plume, *J. Petrol*., *51*, 1507–1540.

Greene, A. R., M. O. Garcia, D. Weis, G. Ito, M. Kuga, J. Robinson, and S. Yamasaki (2010), Low-productivity Hawaiian volcanism between Kauai and Oahu, *Geochem. Geophys. Geosyst.*, *11*, Q0AC08, doi:10.1029/2010GC003233.

Hanano, D., D. Weis, J. S. Scoates, S. Aciego, and D. J. DePaolo (2010), Horizontal and vertical zoning of heterogeneities in the Hawaiian mantle plume from the geochemistry of consecutive postshield volcano pairs: Kohala-Mahukona and Mauna Kea-Hualalai, *Geochem. Geophys. Geosyst.*, *11*, Q01004, doi:10.1029/2009GC002782.

Hauri, E. H. (1996), Major-element variability in the Hawaiian mantle plume, *Nature*, *382*, 415–419.

Hirschmann, M. M. (2000), Mantle solidus: Experimental constraints and the effects of peridotite composition, *Geochem. Geophys. Geosyst.*, *1*, 1042, doi:10.1029/2000GC000070.

Hirschmann, M. M., T. Kogiso, M. B. Baker, and E. M. Stolper (2003), Alkalic magmas generated by partial melting of garnet pyroxenite, *Geology*, *31*(6), 481–484.

Huang, S., and F. A. Frey (2005), Recycled oceanic crust in the Hawaiian plume: Evidence from temporal geochemical variations within the Koolau Shield, *Contrib. Mineral. Petrol.*, *149*, 556–575.

Huang, S., F. A. Frey, J. Blichert-Toft, R. V. Fodor, G. R. Bauer, and G. Xu (2005), Enriched components in the Hawaiian plume: Evidence from Kahoolawe Volcano, Hawaii, *Geochem. Geophys. Geosyst*., *6*, Q11006, doi:10.1029/2005GC001012.

Jackson, E. D., and T. L. Wright (1970), Xenoliths in the Honolulu volcanic series, Hawaii, *J. Petrol*., *11*, 405–430.

Jackson, E. D., E. A. Silver, and G. B. Dalrymple (1972), Hawaiian-Emperor Chain and its relation to Cenozoic circumpacific tectonics, *Geol. Soc. Am. Bull.*, *83*, 601–618.

Keshav, S., and G. Sen (2001), Majoritic garnets in Hawaiian Xenoliths: Preliminary results, *Geophys. Res. Lett.*, *28*, 3509–3512.

Keshav, S., and G. Sen (2004), The depth of magma fractionation in the oceanic mantle: Insights from garnet bearing xenoliths from Oahu, Hawaii, *Geophys. Res. Lett.*, *31*, LO4611, doi:10.1029/2003GL018990.

Keshav, S., G. Sen, and D. C. Presnall (2007), Garnet bearing xenoliths from Salt Lake Crater, Oahu, Hawaii: High pressure fractional crystallization in the oceanic mantle, *J. Petrol.*, *48*, 1681–1724.

Keshav, S., G. H. Gudfinnsson, G. Sen, and Y. Fei (2004), High pressure melting experiments on garnet clinopyroxenite and the alkalic to tholeiitic transition in ocean island basalts, *Earth Planet. Sci. Lett.*, *223*, 365–379.

Kogiso, T., M. M. Hirschmann, and D. J. Frost (2003), High-pressure partial melting of garnet pyroxenite: Possible mafic lithologies in the source of ocean island basalts, *Earth Planet. Sci. Lett.*, *216*, 603–617.

Lassiter, J. C., and E. H. Hauri (1998), Osmium-isotope variations in Hawaiian lavas: Evidence for recycled oceanic lithosphere in the Hawaiian plume, *Earth Planet. Sci. Lett.*, *164*, 483–496.

Lassiter, J. C., E. H. Hauri, P. W. Reiners and M. O. Garcia (2000), Generation of Hawaiian post-erosional lavas by melting of a mixed lherzolite/pyroxenite source, *Earth Planet. Sci. Lett.*, *178*, 269–284.

Leeman, W. P., D. C. Gerlach, M. O. Garcia, and H. B. West (1994), Geochemical variations in lavas from Kahoolawe volcano, Hawaii—Evidence for open system evolution of plume-derived magmas, *Contrib. Mineral. Petrol.*, *116*(1-2), 62–77.

Li, X., R. Kind, X. Yuan, I. Wolbern, and W. Hanka (2004), Rejuvenation of the lithosphere by the Hawaiian plume, *Nature*, *427*, 827–829.

Lipman, P. W., D. Clague, J. G. Moore, and R. T. Holcomb (1989), South Arch volcanic field-newly identified young lava flows on the sea floor south of the Hawaiian ridge, *Geology*, *17*, 611–614.

Liu, T.-C., and D. C. Presnall (2000), Liquidus phase relations in the system CaO–MgO–Al2O3–SiO2 at 2.0 GPa: Applications to basalt fractionation, eclogites, and igneous sapphirine, *J. Petrol.*, *41*, 3–20.

Mahoney, J. J., S. J. M., M. D. Kurz, J. D. Macdougall, K. J. Spencer, and G. W. Lugmair (1994), Isotope and trace element characteristics of a super-fast spreading ridge: East Pacific rise, 13–23°S, *Earth Planet. Sci. Lett.*, *121*, 173–193.

Manhès, G., C. J. Allègre, and A. Provost (1984), U-Th-Pb systematics of Juvinas, *Geochim. Cosmochim. Acta*, *48*, 2247–2274.

Marske, J. P., A. J. Pietruszka, D. Weis, M. O. Garcia, and J. M. Rhodes (2007), Rapid passage of a small-scale mantle heterogeneity through the melting regions of Kilauea and Mauna Loa Volcanoes, *Earth Planet. Sci. Lett.*, *259*(1–2), 34–50, doi:10.1016/j.epsl.2007.04.026.

McDonough, W. F., and S.-s. Sun (1995), The composition of the earth, *Chem. Geol.*, *120*, 223–253.

Milholland, C. S., and D. C. Presnall (1998), Liquidus phase relations in the CaO-MgO-Al_2O_3-SiO_2 systme at 3.0 GPa: The aluminus pyroxene thermal devide and high-pressure fractionation of picritic and komatiic magmas, *J. Petrol.*, *39*, 3–27.

Moore, J. G., and D. Clague (2004), Hawaiian submarine manganese-iron oxide crusts—A dating tool?, *GSA Bull.*, *116*, 337–347.

Morgan, W. J. (1971), Convection plumes in the lower mantle, *Nature*, *230*, 42–43.

Morimoto, N. (1988), Nomenclature of pyroxenes, *Am. Mineral.*, *73*, 1123–1133.

Mukhopadhyay, S., J. C. Lassiter, K. A. Farley, and S. W. Bogue (2003), Geochemistry of Kauai shield-stage lavas: Implications for the chemical evolution of the Hawaiian plume, *Geochem. Geophys. Geosyst.*, *4*(1), 1009, doi:10.1029/2002GC000342.

Müller, R. D., W. R. Roest, J.-Y. Royer, L. M. Gahagan, and J. G. Sclater (1997), Digital isochrons of the world's ocean floor, *J. Geophys. Res.*, *102*, 3211–3214, doi:10.1029/96JB01781.

Munker, C., S. Weyer, E. Scherer, and K. Mezger (2001), Separation of high field strength elements (Nb, Ta, Zr, Hf) and Lu from rock samples for MC-ICPMS measurements, *Geochem. Geophys. Geosyst.*, *2*, 1064, doi:10.1029:2001GC000183.

Nickel, K. G., and D. H. Green (1985), Empirical geothermobarometry for garnet peridotites and implications for the nature of the lithosphere, kimberlites and diamonds, *Earth Planet. Sci. Lett.*, *73*, 158–170.

Nimis, P., and H. Grutter (2010), Internally consistent geothermometers for garnet peridotites and pyroxenites, *Contrib. Mineral. Petrol.*, *159*, 411–427.

Niu, Y. L., K. D. Collerson, R. Batiza, J. I. Wendt, and M. Regelous (1999), Origin of enriched-type mid-ocean ridge basalt at ridges far from mantle plumes: The East Pacific Rise at 11 degrees 20 ' N, *J. Geophys. Res.*, *104*, 7067–7087.

Norman, M. D., and M. O. Garcia (1999), Primitive magmas and source characteristics of the Hawaiian plume: Petrology and geochemistry of shield picrites, *Earth Planet. Sci. Lett.*, *168*, 27–44.

Norman, M. D., M. O. Garcia, and V. C. Bennet (2004), Rhenium and chalcophile elements in basaltic glasses from Ko'olau and Molokai volcanoes: Magmatic outgassing and composition of the Hawaiian plume, *Geochim. Cosmochim. Acta*, *68*, 3761–3777.

Nowell, G. M., P. D. Kempton, S. R. Noble, J. G. Fitton, A. D. Saunders, J. J. Mahoney, and R. N. Taylor (1998), High precision Hf isotope measurements of MORB and OIB by thermal ionisation mass spectrometry: Insights into the depleted mantle, *Chem. Geol.*, *149*(3–4), 211–233, doi:10.1016/s0009–2541(98)00036-9.

Ozawa, A., T. Tagami, and M. O. Garcia (2005), Unspiked K-Ar dating of the Honolulu rejuvenated and Ko'olau shield volcanism on O'ahu, Hawai'i, *Earth Planet. Sci. Lett.*, *232*, 1–11.

Pertermann, M., M. M. Hirschmann, K. Hametner, D. Gunther and M. W. Schmidt (2004), Experimental determination of trace element partitioning between garnet and silica-rich liquid during anhydrous partial melting of MORB-like eclogite, *Geochem. Geophys. Geosyst.*, *5*, Q05A01, doi:10.1029/2003GC000638.

Pietruszka, A. J., M. J. Keyes, J. A. Duncan, E. H. Hauri, R. W. Carlson and M. O. Garcia (2011), Excesses of seawater-derived 234U in volcanic glasses from Loihi Seamount due to crustal contamination, *Earth Planet. Sci. Lett.*, *304*(1–2), 280–289, doi:10.1016/j.epsl.2011.02.018.

Presti, A. A. (1982), The petrology of pyroxenite xenoliths from Kaula island, Hawaii, MSc thesis, Dept. of Geol. and Geophys. Univ. of Hawaii.

Priestley, K., and F. Tilmann (1999), Shear-wave structure of the lithosphere above the Hawaiian hot spot from two-station Rayleigh wave phase velocity measurements, *Geophys. Res. Lett.*, *26*(10), 1493–1496.

Prinzhofer, A., E. Lewin, and C. J. Allègre (1989), Stochastic melting of the marble cake mantle: Evidence from local study of the East Pacific Rise at 12°50'N, *Earth Planet. Sci. Lett.*, *92*, 189–206.

Regelous, M., Y. Niu, J. I. Wendt, R. Batiza, A. Greig, and K. D. Collerson (1999), Variations in the geochemistry of magmatism on the East Pacific Rise at 10 degrees 30' N since 800 ka, *Earth Planet. Sci. Lett.*, *168*(1-2), 45–63.

Reiners, P. W., and B. K. Nelson (1998), Temporal-compositional-isotopic trends in rejuvenated magmas of Kauai, Hawaii, and implications for mantle melting processes, *Geochim. Cosmochim. Acta*, *62*, 2347–2368.

Ribe, N. M., and U. R. Christensen (1999), The dynamical origin of Hawaiian volcanism, *Earth Planet. Sci. Lett.*, *171*, 517–531.

Roden, M. F., F. A. Frey, and D. A. Clague (1984), Geochemistry of tholeiitic and alkalic lavas from the Koolau Range, Oahu, Hawaii: Implications for Hawaiian volcanism, *Earth Planet. Sci. Lett*., *69*, 141–158.

Salters, V. J. M., and A. Zindler (1995), Extreme $^{176}Hf/^{177}Hf$ in the sub-oceanic mantle, *Earth Planet. Sci. Lett.*, *129*, 13–30.

Salters, V. J. M., and W. M. White (1998), Hf isotope constraints on mantle evolution, *Chem. Geol.*, *145*, 447–460.

Salters, V. J. M., J. E. Longhi, and M. Bizimis (2002), Near mantle solidus trace element partitioning at pressures up to 3.4 GPa, *Geochem. Geophys. Geosyst.*, *3*, 1–23, doi:10.1029/2001GC000148.

Salters, V. J. M., J. Blichert-Toft, A. Sachi-Kocher, Z. Fekiacova, and M. Bizimis (2006), Isotope and trace element evidence for depleted lithosphere being sampled by the enriched Ko'olau basalts, *Contrib. Mineral. Petrol.*, *151*, 297–312.

Salters, V. J. M., S. Mallick, S. R. Hart, C. E. Langmuir, and A. Stracke (2011), Domains of depleted mantle: New evidence from hafnium and neodymium isotopes, *Geochem. Geophys. Geosyst.*, *12*, Q08001, doi:10.1029/2011GC003617.

Sen, G. (1987), Xenoliths associated with the Hawaiian hot spot, in *Mantle xenoliths*, edited by P. H. Nixon, pp. 359–375, John Wiley, New York.

Sen, G. (1988), Petrogenesis of spinel lherzolite and pyroxenite suite xenoliths from the Koolau shield, Oahu, Hawaii: Implications for petrology of the post-eruptive lithosphere beneath Oahu, *Contrib. Mineral. Petrol*., *100*, 61–91.

Sen, I. S., M. Bizimis, and G. Sen (2010), Geochemistry of sulfides in Hawaiian garnet pyroxenite xenoliths: Implications for highly siderophile elements in the oceanic mantle, *Chem. Geol.*, *273*(3-4), 180–192.

Sen, I. S., M. Bizimis, G. Sen, and S. Huang (2011), A radiogenic Os component in the oceanic lithosphere? Constraints from Hawaiian pyroxenite xenoliths, *Geochim. Cosmochim. Acta*, *75*, 4899–4916.

Sherrod, D. R., J. M. Sinton, S. E. Watkins, and K. M. Brunt (2007), Geologic map of the State of Hawaii, *U.S. Geol. Surv*. Open-File Rep., 2007-1089, http://pubs.usgs.gov/of/2007/1089/.

Sims, K. W. W., et al. (2003), Aberrant youth: Chemical and isotopic constraints on the origin of off-axis lavas from the East Pacific Rise, 9 degrees-10 degrees N, *Geochem. Geophys. Geosyst*., *4*, 8621, doi:10.1029/2002GC000443.

Sleep, N. (1990), Hotspots and mantle plumes: Some phenomenology, *J. Geophys. Res.*, *95*, 6715–6736.

Sobolev, A. V., A. W. Hofmann, S. V. Sobolev, and I. K. Nikogosian (2005), An olivine-free mantle source of Hawaiian shield basalts, *Nature*, *434*, 590–597.

Staudigel, H. A., A. Zindler, S. R. Hart, T. Leslie, C.-Y. Chen, and D. Clague (1984), The isotope systematics of a juvenile intraplate volcano: Pb, Nd and Sr isotope ratios of basalts from Loihi Seamount, Hawaii, *Earth Planet. Sci. Lett*., *69*, 13–29.

Stille, P., D. M. Unruh, and M. Tatsumoto (1983), Pb, Sr, Nd and Hf isotopic evidence of multiple sources for Oahu, Hawaii basalts, *Nature*, *304*, 25–29.

Stracke, A., V. J. M. Salters, and K. W. W. Sims (1999), Assessing the presence of pyroxenite in the source of Hawaiian basalts: Hafnium-Neodymium-Thorium isotope evidence, *Geochem. Geophys. Geosyst.*, *1*, 1006, doi:10.1029/1999GC000013.

Tanaka, R., A. Makishima, and E. Nakamura (2008), Hawaiian double volcanic chain triggered by an episodic involvement of recycled material: Constraints from temporal Sr–Nd–Hf–Pb isotopic trend of the Loa-type volcanoes, *Earth Planet. Sci. Lett.*, *265*(3–4), 450–465, doi:10.1016/j.epsl.2007.10.035.

Tibbetts, N. J., M. Bizimis, M. Longo, S. Keshav, V. J. M. Salters, and C. A. McCammon (2010), Apparent oxygen fugacity structure beneath Oahu, Hawaii, *Geochim. Cosmochim. Acta*, *74*(12), A1045.

Todt, W., R. A. Cliff, A. Hanser, and A. W. Hofmann (1996), Evaluation of a $^{202}Pb+^{205}Pb$ double spike for high precision lead isotope analyses, in *Earth Processes: Reading the Isotopic Code*, Geophys. Monogr. Ser., vol 95, edited by A. Basu and S. Hart, pp. 429–437, AGU, Washington, D.C.

Vervoort, J. D., T. Plank, and J. Prytulak (2011), The Hf–Nd isotopic composition of marine sediments, *Geochim. Cosmochim. Acta*, *75*(20), 5903–5926, doi:10.1016/j.gca.2011.07.046.

Waggoner, D. G. (1993), The age and alteration of central Pacific oceanic crust near Hawaii site 843, *Proc. Ocean Drill. Program Sci. Results*, *136*, 119–132.

Walter, M. J. (1998), Melting of garnet peridotite and the origin of komatiite and depleted lithosphere, *J. Petrol.*, *39*, 29–60.

Wanless, V. D., M. O. Garcia, F. A. Trusdell, J. M. Rhodes, M. D. Norman, D. Weis, D. J. Fornari, M. D. Kurz, and H. Guillou (2006), Submarine radial vents on Mauna Loa Volcano, Hawai'i, *Geochem. Geophys. Geosyst*., *7*, Q05001, doi:10.1029/2005GC001086.

Weis, D., M. O. Garcia, J. M. Rhodes, M. Jellinek, and J. S. Scoates (2011), Role of the deep mantle in generating the compositional asymmetry of the Hawaiian mantle plume, *Nat. Geosci.*, *4*(12), 831–838.

Wendt, I. J., M. Regelous, Y. Niu, R. Hekinian, and K. D. Collerson (1999), Geochemistry of lavas from the Garrett transform Fault: Insights into mantle heterogeneity beneath the eastern Pacific, *Earth Planet. Sci. Lett.*, *173*, 271–284.

White, R. W. (1966), Ultramafic inclusions in basaltic rocks from Hawaii, *Contrib. Mineral. Petrol.*, *12*, 245–314.

White, W. M., A. W. Hofmann, and H. Puchelt (1987), Isotope geochemistry of Pacific mid-ocean ridge basalts, *J. Geophys. Res.*, *92B*, 4881–4893.

White, W. M., F. Albarède, and P. Telouk (2000), High-precision analysis of Pb isotope ratios by multi-collector ICP-MS, *Chem. Geol.*, *167*(3-4), 257–270.

Woodland, A. B. (2009), Ferric iron contents of clinopyroxene from cratonic mantle and partitioning behaviour with garnet, *Lithos*, *112*, 1143–1149.

Xu, G., F. A. Frey, D. A. Clague, D. Weis, and M. H. Beeson (2005), East Molokai and other Kea-trend volcanoes: Magmatic processes and sources as they migrate away from the Hawaiian hot spot, *Geochem. Geophys. Geosyst.*, *6*, Q05008, doi:10.1029/2004GC000830.

Xu, G., F. A. Frey, D. A. Clague, W. Abouchami, J. Blichert-Toft, B. Cousens, and M. Weisler (2007), Geochemical characteristics of West Molokai shield- and postshield-stage lavas: Constraints on Hawaiian plume models, *Geochem. Geophys. Geosyst.*, *8*, Q08G21, doi:10.1029/2006GC00155.

Yang, H.-J., F. A. Frey, and D. A. Clague (2003), Constraints on the source components of lavas forming the Hawaiian north Arch and Honolulu volcanics, *J. Petrol.*, *44*, 603–627.